Structure, environmental patterns and impact of expected climate change in natural beech-dominated forests in the Cantabrian Range (NW Spain)

Javier Castaño-Santamaría[1 2 3], Carlos A. López-Sánchez[1], José Ramón Obeso[2], Marcos Barrio-Anta[1*]

[1] SMartForest Group, Department of Biology of Organisms and Systems, Oviedo University, Mieres, Spain.

[2] UMIB-Research Unit of Biodiversity (UO, CSIC, PA), Oviedo University, Mieres, Spain.

[3] Directorate General for Cadastre, Ministry of Finance, Regional Office of Asturias, Oviedo, Spain.

* Corresponding author. Address: Polytechnic School of Mieres, E-33600 Mieres, Asturias, Spain. Tel.: +34 985 45 80 05; E-mail address: barriomarcos@uniovi.es (M. Barrio-Anta).

Declaration of interest: none.

Abstract

The European beech (*Fagus sylvatica* L.) occurs in the Cantabrian Range (NW Spain), at the southwestern limit of the wide distribution area of the species in Europe, forming relatively unmanaged forests of high biodiversity value. In this study, we measured three-dimensional positions, diameter at breast height and height of all the trees present in 112 inventory plots established in beech-dominated forests in the north-western Cantabrian Range, in which hemispherical photographs were taken and a detailed floristic inventory was carried out. In addition, we measured 56 spatially continuous environmental variables in each plot to enable examination of environmental patterns in structural features and prediction of the effects of climate change. Forest structure was analyzed by using indices that evaluated spatial tree distribution, plant richness and tree species diversity, diversity of tree dimensions and vertical structure, stand density and average tree size, standing deadwood, canopy geometry and light regime. The stands exhibited a moderate clustered spatial arrangement at young stages, becoming more regular as they matured. The stands are generally monospecific, with low plant richness, never monostratified, with very close canopies, greater variation in diameter than in height and are usually overstocked. Only 25% of the stands included some standing dead trees. Random Forest models were used to describe structural features as a function of environmental variables. Although some of the models were complex and included many predictor variables, they revealed some interesting patterns. Thus, we found that spatial tree distribution was only related to lithostratigraphy, and tree species richness and vertical structure were related to isothermality. Shrub and herbaceous richness were related to soil pH and several thermal variables, while intermingling of tree species was mainly explained by soil-related variables. Climatic variables explained differences in tree diameter, whereas edaphic variables were more important for predicting differences in tree height. Stocking level was mainly related to soil variables, while dominant height was related to thermal variables and standing dead wood to climatic variables. Projections under the moderate RCP 4.5 and pessimistic RCP 8.5 climate change scenarios predict a shift in beech forests towards increased shrub and plant richness and species diversity, but also increased stocking level and standing deadwood basal area. These findings appear to confirm a drastic reduction in the suitable habitat for beech in the

region (deterioration of future growth conditions), which could anticipate a loss of competitive advantage over other species and indicate a shift in this beech-dominated forest to more resilient mixed stands.

Keywords

Fagus sylvatica L.; spatial patterns; species diversity; tree dimensions; stand density; deadwood.

1. Introduction

Forests are dynamic ecosystems in which trees grow, propagate, compete for essential resources and die. None of these processes are independent from the structural composition of the forest (Gadow et al., 2011) and they interact in a complicated way (both act as causes and effects), making it difficult to disentangle them (Pommerening et al., 2011). Forest structure determines the distribution of micro-climatic conditions (e.g. temperature, vapour concentration and radiation regime), the availability of resources, energy and nutrient fluxes, primary productivity and the formation of habitat niches, and it thus directly or indirectly determines the biological diversity, health and ecological stability of the forest community (Pommerening, 2002; Gadow et al., 2011). Short-term processes, in turn, modify the structure in the long term (Pommerening, 2007).

Forest structure usually refers to the way in which the main tree attributes are expressed within a forest ecosystem. More specifically, according to Gadow (1999), forest structure can be defined by the spatial distribution of the tree positions (both horizontally and vertically), by the spatial mixing of the different tree species and by the spatial arrangement of the tree dimensions. In addition, an important stand attribute such as density may also be considered a structural feature from the broad scale analysis of the forest (Pretzsch, 2009), because it refers to a quantitative measure of the level of site utilization and is closely related to stand growth and yield (Burkhart and Tomé, 2012). Moreover, other parameters such as the presence and size of canopy gaps, the canopy architecture, the presence and abundance of understory vegetation or standing deadwood and woody debris are also important elements of the structure (e.g. Harmon et al., 1986; Montgomery and Chazdon, 2001).

Forest structure is thus both a product of and a factor involved in ecosystem processes and biological diversity. Information about forest structure can thus help with the following: i) understanding the history, function and future of the forest ecosystem; ii) comparison of managed and unmanaged stands; and iii) establishing a basis for the analysis of forest ecosystem disturbance (e.g. by fire, wind or snow damage), including silvicultural options (Pretzsch, 1997; 1998; Gadow et al., 2011). This type of information is very important for implementing sustainable forest management plans or for biodiversity conservation purposes, under uncertain future management and climate scenarios. Until now, various techniques have been used to explore some features of forest structure as a function of environmental variables (e.g. Silva-Flores et al., 2014; Vilanova et al., 2018). However, in recent decades, the exponential increase in available data (big data) and the use of sophisticated statistical tools such as “machine learning” and “deep learning” techniques have enabled hidden patterns to be uncovered (e.g. Liu et al., 2018; Choudhury et al., 2021).

Common beech (*Fagus sylvatica* L.) is the most widely distributed of all *Fagus* species and the most abundant broadleaved forest tree in Europe (Fang and Lechowicz, 2006). As a result of the abundance of beech forests, their structure has been widely investigated, but the spatial and temporal variation due to underlying environmental patterns and expected climate change have scarcely been considered. Thus, previous studies have analyzed tree position, species diversity and tree dimension diversity (e.g. Pommerening, 2002; von Oheimb et al., 2005), the spatial distribution of dead trees (e.g. Vasile et al., 2017), canopy geometry and light regime (e.g. Collet et al., 2001), and some have even differentiated between managed and unmanaged stands (e.g. Bílek et al., 2011; Lombardi et al., 2012) and also pure and mixed stands (e.g. Petritan et al., 2012). However, no previous studies have analyzed all of these structural elements together or how they could be affected by climate change.

Beech is considered a climax species in the study area (the Cantabrian Range, NW Spain), where it is restricted to slopes of elevation higher than 600 m above sea level. These forests form part of the habitats of endangered and emblematic species such as the Cantabrian capercaillie and the brown bear, leading to their inclusion in protected areas relatively unaffected by human influence. As result of climate change, these areas have undergone a gradual increase in temperature and potential evapotranspiration, together with a decrease in precipitation in recent decades (Rubio-Cuadrado et al., 2018). In addition, more frequent and severe drought events are expected in the future (e.g. IPCC, 2013). Several studies have already demonstrated the impact of climate change on the current distribution and productivity of beech forests in Europe (e.g. Kramer et al., 2010; Falk and Hempelmann, 2013), but the foreseeable effects on stand structure remain unclear.

Occurrence, abundance, site productivity and stand structure – and the temporal and spatial variations in these – are of major interest for the purposes of biodiversity conservation for particular tree species. Some of our previous research has focused on species occurrence and site quality in the area (Castaño-

Santamaría et al., 2019), but not on abundance and structure. In addition to describing the structure of beech forest, the underlying hypothesis for this research was that we would be able to detect and model patterns in environmental variables and structural features in order to forecast the effects of climate change. Thus, the overall aims of the present study were to characterize the current structure of natural beech-dominated forests in the Cantabrian Range and to analyze environmental patterns to enable prediction of spatial variations in structure and its foreseeable future evolution due to climate change. The following specific objectives were necessary to achieve the overall goals: *i*) to analyze the current structure by means of quantitative indices and to determine the correlations between indices to explore the possibility of predicting more difficult-to-determine indices from others and also to enhance interpretation of structural features; *ii*) to identify the strongest patterns in structural features for building predictive models to relate these to environmental variables; and *iii*) to project these models in space and time under different forecasted climate change scenarios.

2. Materials and methods

2.1. Study area

The Cantabrian Range represents the western limit of the European Mountain System; it is a transitional zone between the Eurosiberian and Mediterranean regions in the Iberian Peninsula and exhibits considerable asymmetry between the northern and southern sides (Díaz and Fernández, 1987). Originated from Alpine orogeny, ancient Paleozoic rocks predominate in the central axis, flanked by Mesozoic and Tertiary rocks in the lower mountains of the eastern zone (IGME, 2015a). In the context of European biogeography, the Cantabrian Range forms part of the Atlantic climate region, with an annual average temperature of ca. 9 ºC and an average precipitation of ca. 1200 mm, distributed uniformly throughout the year. Beech (*Fagus sylvatica* L.) stands are the dominant forest in terms of surface area on the northern side, followed by birch (*Betula* spp.) and oak forests (*Quercus petraea* (Matt.) Liebl. and *Quercus robur* L.) (García et al., 2005).

2.2. Data collection

Six different types of data were considered in this study: *i*) tree size measurements, *ii*) tree positions in a three-dimension system, which together with previous data were used to study structure, *iii*) hemispherical photographs, used to study canopy structure and gap light transmission indices, *iv*) floristic inventory of the accessory vegetation present in the forests, *v*) data on current spatial environmental variables, used to analyze the relationship with structural features and to map them, and *vi*) future climatic data projections under different emission scenarios, used to predict the impact of climate change on structural features.

2.2.1. Field sampling

A total of 112 permanent sample plots were established in natural beech-dominated forests throughout the north-western Cantabrian Range (NW Spain) in 2010 and 2011 (Figure 1), to cover the existing range of stand structures, stand densities and site qualities. The plots ranged in size from 400 to 3600 m^2, depending on stand density, in order to achieve a minimum of 30 trees per plot. Management input in the sampled stands has been minimal (i.e. unlogged for at least 50 years) because these forests are located in environmentally protected areas. As a result, inter-tree interactions are relatively unmodified by human intervention. These plots were used as the sources of data types *i*), *ii*), *iii*) and *iv*) outlined above.

Detailed analysis of forest structure requires expansion of measurements traditionally made in forest inventories. Thus, in each plot, diameter at breast height, total height and other descriptive variables of each tree (e.g. species, if they were alive or dead, etc.) were recorded. All of the trees were mapped in three dimensions using an electronic theodolite. A floristic inventory of the accessory vegetation was also carried out, identifying the species and their abundance and average height.

Finally, hemispherical photography was used to assess canopy structure, leaf area index and light conditions, because of the complexity of measuring canopy characteristics directly (Hale and Edwards, 2002; Jonckheere et al., 2004). Three hemispherical photographs were taken in the centre and in the northeast and southwest corners of the plot. Images were acquired using a Nikon FC-E9 fish-eye lens attached to a Nikon P7000 digital camera (Nikon Inc., Tokyo, Japan). The camera body was located approximately 0.5 m above the ground (to simulate the understory vegetation lighting conditions without interference of that vegetation). It was pointed upwards using a double bubble level located in the tripod, and it was orientated to magnetic north. Photographs were taken under uniform sky conditions in the absence of direct sun radiation, because of the low scattering coefficients of leaves under these conditions and even with illumination of the sky (Rich, 1990).

2.2.2. Collection of spatial environmental variables

Three types of environmental parameters were considered for analyzing the environmental patterns and for spatial modelling: terrain, climate and soil variables. A total of 56 variables were available for analysis (Table 1).

Terrain variables (seven topographic, one hydrographic and three potential incoming solar radiation) were extracted from the 5 m resolution digital elevation model (DEM) provided by the Spanish National Plan for Aerial Orthophotography (PNOA; www.pnoa.ign.es). Gridded data were obtained for all climate variables with a 30 arc-second resolution (approximately 800 m) from WorldClim

(Hijmans et al., 2005). A total of 19 climatic variables were considered. Sixteen soil variables were compiled from LUCAS (Ballabio et al., 2019) and SoilGrids250m (Hengl et al., 2017), which provide a collection of updatable soil properties and world classification maps at 500 m and 250 m spatial resolution, respectively. Soil type and group were compiled from the European soil database (ESDB) v2.0. Lithostratigraphic type and permeability were obtained from the Spanish Stratigraphic Map (SSM) scale 1:200,000, and Geology from the Spanish Geological Map (SGM) scale 1:1,000,000 (IGME, 2015a; 2015b). All climate, soil and topography variable raster grids were resampled at 250 m resolution.

To predict the effect of different climate change scenarios on the structural features of beech forest, we used the Global Climate Models (GCMs) for 2050 and 2070 based on the CMIP5 model of the IPCC 5th Assessment Report (http://www.worldclim.org/CMIP5). Bioclimatic predictions for two opposing scenarios of representative concentration pathways (RCP) were considered. The first, "moderate scenario" (RCP 4.5) assumes a CO_2 concentration of 650 ppm and an increase of 1.0–2.6°C by 2100 (Thomson et al., 2011), whereas the second, "pessimistic scenario" (RCP 8.5) considers a CO_2 concentration of 1,350 ppm (Riahi et al., 2011) and a temperature increase of 2.6–4.8°C by 2100 (IPCC, 2013; Harris et al., 2014).

2.3. Forest structural features and indices analyzed

In this study, six structure features were analyzed: *i*) spatial tree distribution, *ii*) plant richness and tree species diversity, *iii*) diversity of tree dimensions and vertical structure, *iv*) stand density and average tree size, *v*) standing deadwood and *vi*) canopy geometry and light regime. For this purpose, we used stand-based and tree-based indices. Stand-based indices provide a unique value for each plot, whereas tree-based indices yield an index value for each tree of the stand based on information from neighbouring trees and the subject itself, so that study of the distribution is more precise than with the arithmetic mean values (Pommerening, 2006).

For analysis of the three first structural features mentioned above, a total of 22 indices (13 stand-based and 9 tree-based indices) were considered (see Table 2). These indices were estimated by taking into account the edge-correction proposed by Pommerening and Stoyan (2006). Neighbour selection may result in trees outside plot boundaries being identified as neighbours. Edge correction was therefore required for unbiased estimation of spatial variables. This consists of fixing a strip of variable width in each plot, so that those trees closest to the sides of the plot are located in this strip and are taken into account in calculating the distance-dependent indices of the rest of the trees, but for which these indices are not calculated (Pommerening and Stoyan, 2006).

In addition, 9 indices were used to characterize standing deadwood (2 indices) (Table 2) and canopy geometry and light regime (7 indices).

2.3.1. Spatial tree distribution

The horizontal tree distribution patterns were defined from the distances between trees to determine whether the pattern of tree locations is clumped or is described by a regular, random or Poisson distribution (with areas of lower or higher density), or some combination of these. One stand-based structure index (Aggregation Index, *R*) and two tree-based indices (Uniform Angle index (*W*) and Mean Directional index (*MDI*)) were used for this purpose. The Aggregation index developed by Clark and Evans (1954) compares the observed average distance of a tree to its nearest neighbour and the expected average distance between trees in a completely spatially random tree distribution. This index can provide a first general impression of the structure of a forest, but it cannot be used to describe the large variety of spatial arrangements (Zenner and Hibbs, 2000). As a single-tree based alternative to the Aggregation index, Gadow et al. (1998) developed the Contagion index to define the degree of regularity of the spatial distribution of the four trees nearest to a reference tree *i*. The index is based on classification of the angles between these four neighbours. As a reference, the standard angle α_0, which is expected in a regular point distribution, was fixed at 72º according to Hui and Gadow (2002). The mean directional index (Corral-Rivas, 2006) is defined as the sum of the unit vectors from the reference tree *i* to its *n* nearest neighbours and represents the spatial arrangement of trees. In this study, $n = 4$ nearest neighbours.

2.3.2. Plant richness and tree species diversity

To evaluate plant diversity, three different features were considered: species richness (shrubs, herbaceous plants and trees), tree species diversity and tree species intermingling. Species richness refers to the number of species present in the stand. By contrast, species diversity also considers the number of species and their frequency, and the stand can be described as pure or as a two-species or multiple-species mixture. Intermingled tree species define the degree of spatial segregation of the tree species mixture in a stand (mixture of individual tree species or a mixture by groups, clusters, rows or patches). In addition to the tree, shrub and herbaceous plant richness, three stand-related indices (Segregation, Shannon and Simpson indices) and one tree-related index (Mingling index) were used to characterize this structural feature.

The Segregation index developed by Pielou (1977) (*S*) provides a spatially explicit measure for tree species diversity which considers the ratio of the observed probability that the reference tree and its nearest neighbour belong to different species, along with the same probability for completely randomly distributed or independent species attributes. The Shannon (*H'*) and Simpson (*D*) indices are both spatially inexplicit measures of forest species diversity (Shannon and Weaver, 1949; Simpson, 1949). The Shannon index is defined as the probability that a randomly selected tree belongs to the species i, while the Simpson index is interpreted as the probability that two individual trees selected at random belong to different species. However, the Mingling index (M_i) is defined as the proportion of the four nearest neighbours that differ from the reference tree in terms of tree species (Gadow, 1993).

2.3.3. Diversity of tree dimensions and vertical structure

The diversity of tree dimensions considers the spatial arrangement or size mingling of any tree dimensional variable. Differentiation indices (TD_i, TH_i) give the difference in size (diameter or height) of neighbouring trees on a continuous scale and describe the spatial distribution of tree sizes (Füldner, 1995), enabling interpretation of the relationship between the reference tree and its neighbouring trees in relation to competition (Ruprecht et al., 2010). In addition, for calculation of the diameter or height differentiation for a whole forest stand (TDM_i, THM_i), the tree values are summed and divided by the number of trees (Pommerening, 2002). On the other hand, the dominance was proposed as a tree attribute by Hui et al. (1998) to relate the relative dominance of a given tree species to the immediate neighbourhood. It is defined as the proportion of the n nearest neighbours of a given reference tree which are smaller than the reference tree. For height dominance (Uh_i), the elevation at which each tree is growing was included in order to take into account the effect of topography on the vertical stratification of the crowns, which Davies and Pommerening (2008) consider is very significant in this index. The slope of the plot was assumed to be constant, and the elevation at which each tree is growing was determined by triangulation.

The following two indices take the presence of trees species in different height zones into account, as an estimate of the vertical structure of the stand features. The Shannon vertical index (H'_v) (Pretzsch, 1996) considers species proportions separately for tree height zones. According to Pretzsch (1998) these zones range from 0 to 50%, 50 to 80% and 80 to 100% of maximum stand height. On the other hand, the Shannon Stratified index (H'_{str}) (Weber, 2000) enables quantification of the variability in canopy strata in the forest.

2.3.4. Stand density and average tree size

Three widely used stand density indices (number of trees per hectare, basal area and Hart-Becking index (Hart, 1928; Becking, 1953) were considered. In order to qualify stand density values according to some target value (stocking), we used the maximum size-density relationship proposed for the species by Condés et al. (2017) and parametrized for our study region to obtain the maximum density (N_{max}). From this equation, maximum basal area (G_{max}) can also be immediately determined. Beyond this stand density level (maximum density), competition-induced mortality occurs at high rates. The stocking level (*StDeg*), originally developed by Reineke (1933) as the stand density index and defined as the number of trees per hectare of stand (N) divided by N_{max}, provides an estimate of the level of competition within the stand. The stand is considered fully stocked if *StDeg* is between 35% and 60% of N_{max}, overstocked if *StDeg* is greater than 60% of N_{max} and understocked if *StDeg* is lower than 35% of N_{max}, according to the general ranges established by Long (1985). In addition, three stand dimensional indicators (mean height, dominant height and dominant diameter) were also used in this study.

2.3.5. Standing deadwood

Deadwood, a basic component of forest structure, has an important impact on the stability and continuity of forest ecosystems because it plays a fundamental role in the nutrient cycles in forest systems, maintains moisture during dry periods and provides a habitat for numerous organisms (Harmon et al., 1986). In the present study only standing deadwood was assessed though the following two indices: the number of standing dead trees per hectare (to indicate the potential hollow bearing resource) (Franklin et al., 1981), and the basal area of standing dead trees (to indicate the approximate volume of standing dead wood, on the assumption that dead trees were of a similar height) (Tyrrell and Crow, 1994).

2.3.6. Canopy geometry and light regime

Forest light conditions are also closely related to forest structure, influencing tree regeneration, plant growth and plant survival, thus affecting forest understory vegetation patterns and habitat conditions for wildlife (Montgomery and Chazdon, 2001). The hemispherical photographs were analyzed using Gap Light Analyser 2.0 software (GLA) (Frazer et al., 1999), and adjustments were made according to the lens used, the date they were taken and the slope of the plot (see Mason et al., 2012), thus providing advantages over other software. To start the image processing, a threshold level was selected for each photograph to distinguish between visible sky and foliage. In order to minimize the effect of variation in threshold selection, all photographs were analyzed twice by the same person, several days apart, and an average of both analyses was used for all outputs, as recommended by Hale and Edwards (2002).

For each photograph, seven descriptors were calculated. Three of these were related to the canopy geometry: *LAI 4* (effective leaf area index integrated over the zenith angles 0 to 60º), *LAI 5* (effective leaf area index integrated over the zenith angles 0 to 75º) and the site openness (percentage of open sky seen from beneath the forest canopy). The other four descriptors were related to the light regime: direct light (below, direct), diffuse light (below, diffuse) and both types of solar radiation transmitted by the canopy and topographic mask (below, total and as a percentage).

2.4. Data analysis and modelling

Two types of statistical analysis were carried out. First, we determined the correlations between structural indices, to enable *i*) exploration of the possibility of predicting more difficult-to-determine indices from others and *ii*) enhancement of the explanation and interpretation of the structural features analyzed. On the other hand, as the relationship between structural indices and environmental variables may be driven by more complex nonlinear functions, the non-parametric Random Forest approach was also used to model these indices as a function of environmental variables, thus also enabling identification of hidden non-linear patterns. Moreover, this method also enables these indices to be mapped on the territory and forecast of the spatial and temporal variation if they are related to climatic variables. RF analysis was carried out in two steps: *i*) in a preliminary analysis, all structural indices were fitted with RF, and *ii*) the best RF model (or most parsimonious when fitting was similar) within each structural class was selected for a more in-depth analysis.

We used SAS/STAT software (SAS Institute Inc., 2004) to calculate descriptive statistics and to determine correlations between all of the previously calculated structural indices. For this purpose, we used the non-parametric Spearman's correlation coefficient. However, multiple statistical tests were run simultaneously in this analysis, thus increasing the chance of obtaining false positive results (Type I error). In order to solve this problem, the Bonferroni correction was applied (Bonferroni, 1936).

The Random Forest (RF) non-parametric classification and regression approach consists of building an ensemble of decision trees from randomized subsets of predicted and predictor variables (Breiman, 2001). WEKA open source software (Hall et al., 2009) was used to fit the RF algorithm by implementing a wrapper methodology to select the subsample of variables, which usually produces the best results (Zhiwei and Xinghua, 2010). This method selects the subsample of variables by using a learning algorithm as part of the evaluation function. The final fitted models were applied to environmental spatial variables resampled at a 250m x 250m resolution to generate spatially continuous maps. The 10-fold cross-validation approach was used to test the accuracy of the algorithms. This process consists of the following four steps: *i*) splitting the data set into 10 random subsets of roughly the same size; *ii*) fitting the model 10 times, sequentially omitting one subset each time; and *iii*) using each of the fitted models to produce pseudo-independent predictions on the omitted subset, as a good indicator of how well the classifier will perform on unseen data. The pseudo-coefficient of determination (R^2) (Ryan, 1997) and the root mean squared error (*RMSE*) were used to assess the model performance. For implementation of machine learning algorithms, WEKA has an embedded feature ranking technique called the variable importance measure (*VIM*), which was used to guide selection of predictors for the final model. To ensure that values of variable importance were expressed on comparable scales, the *VIM* values were normalized so that they summed to a unit value (normalized importance, VIM_N). After observing that the model performed well, we faced the challenge of correct interpretation. Examining VIM_N is a reasonable first step for interpreting RF models, but it is not sufficient. However, it can be complemented very well with marginal response plots (Choudhury et al., 2021). Constructing such plots enabled us to explore the relationships between the response and the most important predictor variables. These plots represent the predicted outcome of the model (y-axis) as a function of a single environmental variable (x-axis), and all other explanatory variables are held constant at their mean values.

3. Results

The findings are presented for each structural feature, by first describing the characterization and linear correlation with other indices and then by reporting the results of the environmental pattern analysis with RF. To help in the model interpretation, we constructed marginal response curves for variables with the highest VIM_N until reaching an accumulated VIM_N value of at least 75% (curves shown in Figures S1). We generated raster maps (Figure S2) in order to visualize the spatial and temporal variation in the structural features predicted by the RF models.

3.1. Spatial tree distribution

3.1.1. Characterization and linear correlation between indices

According to the aggregation index, approximately two thirds of the plots were characterized by a clustered spatial arrangement of trees. In the remaining third, the trees were regularly distributed, and random distribution was very scarce. Nevertheless, in almost all plots the values of regularity and clustering were moderate (Figure 2). The mean directional index partly corroborates these results, showing a vast majority of plots with a clustered distribution of trees (86%). By contrast, the distribution predicted by the contagion index shows that most plots have random distributions of trees (97%) and only 3% have a clustered distribution. Comparison of these results with the observed values, shows that the contagion index did not perform well for the study plots.

The correlation analysis (Table 4) revealed that regular tree positions appear in forests with the smallest numbers of trees per hectare (–0.3891 for N) and taller trees (0.4163 for H_0 and 0.5535 for H_m) with a spatial separation of species (0.8972 for S), i.e. almost monospecific stands. By contrast, plots with a clustered spatial arrangement have a significantly greater number of trees per hectare than the regular ones, with shorter trees.

3.1.2. Environmental patterns

As the aggregation index produced the most accurate (realistic) results, the best predictive RF model for spatial tree distribution was produced with this index (Table 5) (R^2= 0.16), and the diversity of tree positions was related to some soil properties (lithostratigraphy and texture) (Table 6). Although it did not provide a good fit for predictive purposes, it was valuable for visualization of spatial and temporal variations. The highest values of this index are associated with igneous and metamorphic rocks (granites, slates, quartzites), whereas the lowest values correspond to sedimentary rocks (dolomites, limestones or marls) (Figures S1).

3.2. Plant richness and tree species diversity

3.2.1. Characterization and linear correlation between indices

Regarding plant species richness, a total of 9 tree and 22 shrub and herbaceous species were identified in the study plots. Nevertheless, a maximum of only 4 tree species and up to 12 species of shrubs and herbaceous plants were present in the same plot, although the most common stand type was monospecific (only beech trees) with very low richness of shrubs and herbaceous species (4 or 5 species in the plot).

The segregation index adopted a value higher than zero in all plots, indicating clear spatial separation of species in space. On the other hand, the distance-independent indices (Shannon and Simpson) indicate a clear majority of monospecific stands. In addition, the mingling index revealed a vast majority of monospecific stands. For example, the mode of the mingling index was equal to 0.00 in 105 out of the 112 plots (no mingling) and to 0.25 (weak mingling) in 6 plots. A high modal value of 0.75 of the index, which indicates a high degree of mingling, was only reached in one plot. The proportion of beech basal area relative to the stand basal area was between 46.20% (in the plot with the highest degree of mingling) and 100%, with a mean value of 96.72% (standard deviation = 9.25%). Similar to regular tree positions, the segregation index may indicate that a lower number (–0.3589 for N) of thick, tall trees per hectare (0.3879 for H_0 and 0.4955 for H_m) leads to greater spatial separation of more diverse tree species, with greater height differentiation (Table 4). Moreover, the results indicate that higher tree species richness and species mingling were related to higher strata diversity (0.7501 for TSR and 0.6032 for the mingling index), with greater diameter (0.3701) and height differentiation (0.3554) (which were also correlated with the shrub and herbaceous species richness (0.3877 for *TD*, 0.3740 for *TDM* and 0.3711 for *THM*)).

3.2.2. Environmental patterns

As a result of the feature selection process, three RF models were selected for assessing tree richness, shrub and herbaceous richness and tree species diversity (Tables 5 and 6). RF only retained isothermality as an independent variable for predicting tree species richness (R^2 = 0.25), indicating that higher isothermality values are associated with higher species diversity (see Figure S1). On the other hand, shrub and herbaceous species richness (R^2 = 0.38) is driven by several variables, the most important of which is soil pH, with higher diversity associated with higher pH. In addition, the temperature of the coldest quarter and annual mean temperature accounted for 76% of the variable importance measure (VIM_N) indicating that higher diversity is associated with higher values of both variables (see Figures S1). Finally, RF retained 7 variables for the Shannon diversity index (R^2 = 0.32), but only 5 of those variables already contributed 75% or more of the VIM_N (sand percentage, potassium content, potential incoming radiation in winter solstice, nitrogen content and wetness index). Higher values of predictor variables are associated with higher levels of species intermingling except for wetness index, for which the opposite was found (Figures S1).

3.3. Diversity of tree dimensions and vertical structure

3.3.1. Characterization and correlation between indices

In the analysis of the vertical structure, the Shannon stratified index revealed the existence of various strata in the forest canopy in all plots. Only nine of the plots had two strata with equal relative proportions, which indicates the existence of the dominant and dominated strata. In addition, the Shannon vertical index showed that there were at least two canopy strata in all plots.

The diametric dominance index showed a certain degree of variability. Thus, representing the most frequent values (mode) in each plot (Figure 3) revealed that the number of stands with a larger differentiated dominant group of trees was greater than the number of stands in which these dominant trees are scarcer. However, regarding height dominance, most plots were characterized by mainly co-dominant and moderately dominant and moderately suppressed trees. In other words, significant differences between dominant and dominated strata were only found in only a few plots, corroborating the results obtained with the Shannon stratified index. The differentiation indices provided the same results, indicating very little differentiation in either diameter or height in the vast majority of stands (Table 3, Figure 3).

However, the correlation analysis revealed positive correlations between diameter and height differentiation and dominance (see Table 4). Height differentiation (0.4325) was greater in stands with higher stocking levels. The other results have already reported in the previous sections.

3.3.2. Environmental patterns

The best RF results were obtained for diameter differentiation (R^2=0.27) as a function of environmental variables (Table 6), followed by height differentiation (R^2=0.26) and then by the Shannon vertical index (R^2=0.22). Climatic variables showed greater relative importance in diameter differentiation (potential incoming solar radiation in winter solstice, annual temperature range, isothermality, followed by depth to bedrock…) and the Shannon vertical index (only isothermality). On other hand, edaphic variables showed greater relative importance in height differentiation (cation-exchange capacity, pH, silt content, followed by annual temperature range, isothermality etc.). See Figure S1 for the marginal effect of each variable on the predicted outcomes.

3.4. Density and average tree size indicators

3.4.1. Characterization and correlation between indices

A high level of variability was observed in terms of density and tree size in the study plots. The plots were located throughout the area of distribution of this species in the region and were subjectively selected to represent the existing range of altitude, slope, orientation, etc., resulting in a wide variety of stand densities and site qualities. For example, the number of trees per hectare ranged from 94 to 4200, the basal area ranged from 15.35 to 178.70 m^2 ha^{-1}, the dominant height from 7.15 to 35.90 m and the dominant diameter from 15.30 to 100.12 cm (see Table 2). In other words, although it may be possible to detect certain patterns or trends relative to other structural indices, the same does not apply to these variables. Different results were only obtained for the stocking level, showing that a vast majority of the plots were overstocked (95.91%) and the remaining plots were fully stocked (4.09%). None of the plots were classified as understocked.

The correlation analysis revealed that the number of trees per hectare was not correlated with basal area, indicating that stands may have high basal area due to the presence of many small trees or a few large trees (Table 4). However, as a result of stand development and competition, the number of trees was negatively correlated with mean and dominant height (-0.4827 and -0.5457, respectively), whereas basal area was positively correlated with the same (0.4316 for H_0 and 0.3977 for H_m). Greater density (-0.3973) and tree height indicate relatively higher density (lower Hart-Becking index). Moreover, the stocking level was higher in forests in which a high mingling index value (0.9965) was recorded.

3.4.2. Environmental patterns

Dominant height was the stand dimension variable most strongly related to the environmental variables, which is consistent with the fact that this variable is used to define forest site quality. In the RF model for dominant height (R^2 = 0.509), climate variables contributed most to the model (temperature seasonality, mean temperature of warmest month, mean diurnal range and precipitation seasonality), followed by terrain (slope) and then soil variables.

Among the stand density variables, stocking level is a much more informative variable for stand condition than the simpler number of trees per hectare. The RF model for stocking level yielded a moderate fit to the data (R^2 = 0.22) indicating that this variable is influenced by numerous interrelated variables (16 environmental variables), of which 9 were necessary to yield more than 75% of the accumulated relative importance (Table 6). Edaphic variables (e.g. bulk density, phosphorus and nitrogen content, carbon-nitrogen ratio and cation-exchange capacity) were relatively more important than climatic and terrain variables (e.g. annual mean temperature, plan curvature and wetness index). See Figure S1 for visualization of the marginal effect of each variable on the predicted outcomes.

3.5. Standing deadwood

3.5.1. Characterization and correlation between indices

The amount of standing deadwood observed was very low. Thus, most of the study plots (74.11%) did not have any standing dead trees, 15.18% contained fewer than 50 standing dead trees per hectare, 8.03% had between 50 and 100, and only 3 plots (2.68 %) had more than 100 standing dead trees per hectare. The maximum proportion of dead trees relative to the total number of trees per hectare was 16.6%, while the average proportion was around 5%. Regarding the basal area of standing dead trees, in 53.57% of the plots these trees constituted less than 1% of the total basal area of the plots with standing dead trees, while there were between 1 and 5% in 42.86% of the plots and only 3.57% of them exceed 5%, with a maximum of 6.38% of the total basal area.

Correlations between structural indices (Table 4) showed that forests in which density is excessive were richer in standing dead wood (0.3942 between stocking level and basal area of standing dead trees).

3.5.2. Environmental patterns

The RF deadwood model (for the basal area of the standing dead trees (R^2 = 0.385)) only includes two climatic variables (with 100% relative importance for mean diurnal range) (Table 6). The marginal response curve indicates that greater amounts of standing dead wood are associated with higher values of mean diurnal range until reaching a peak (see Figure S1).

3.6. Canopy geometry and light regime

3.6.1. Characterization and correlation between indices

As previously stated, forest canopy architecture determines the amount and distribution of light in the plots. Slightly higher values can be seen in LAI 4 than in LAI 5 (Table 2), as the latter takes into account trees that are not immediately surrounding the site and which are found outside of the plot footprint (Sánchez-Azofeifa et al., 2017). Below-canopy radiation, i.e. direct, diffuse and total radiation, ranged from 1.14 to 3.58 MJ m^{-2} d^{-1}, from 1.79 to 3.38 MJ m^{-2} d^{-1} and from 2.72 to 6.12 MJ m^{-2} d^{-1}, respectively. Finally, the percentage of total radiation transmitted by the canopy and which reaches the ground (taking the topography into account) ranged from 8.28 to 17.13%.

None of the correlations considered in this part of the study were significant after application of the Bonferroni correction. However, when this correction was not taken into account, the results shown in Table 4 indicate more direct and total radiation below the canopy at lower tree density and that existing trees under these conditions are regularly spatially distributed. In addition, more dead trees imply more gaps (greater canopy openness) and therefore more diffuse radiation below the canopy. Nevertheless, these results should be considered preliminary and must be confirmed.

3.6.2. Environmental patterns

For this type of indices, none of the RF models yielded significant fits.

3.7. Forecasting the effects of climate change on beech forest structure

Although differing in the intensity of change, all of the predicted scenarios coincide in an increase in temperature and a reduction in precipitation in the study area over the next few decades (see Table S1). For example, the annual mean temperature is expected to increase by respectively 17.22% and 20.41% under RCP 4.5 for 2050 and 2070, and by respectively 24.66% and 34.40% under RCP 8.5 for 2050 and 2070. Annual precipitation is expected to decrease by respectively 7.61% and 8.51% under RCP 4.5 for 2050 and 2070, and by respectively 9.84% and 11.73% under RCP 8.5 for 2050 and 2070.

The changes in climate conditions are expected to have significant impacts on the structural features of the beech stands under study. RF models that retained climatic variables as predictors are sensitive to climate change and were used to generate spatially and temporally explicit maps. These maps (Figure S2) enabled us to visualize the expected degree of change in the values of the structural indices under two climate change scenarios (moderate scenario-RCP 4.5 and pessimistic scenario-RCP 8.5) and for two temporal horizons (2050 and 2070). By way of example, the spatially and temporally explicit map of the variation in the standing deadwood basal area is shown in Figure 4.

Climate change is not expected to affect the structural feature “diversity of tree position”, as the RF model did not include any climatic variable as a predictor.

Regarding “plant richness and species diversity”, tree richness would be slightly higher under the RCP 4.5 scenario (moderate scenario) and much lower under the RCP 8.5 scenario (pessimistic scenario). However, as a consequence of less favourable environmental conditions for beech, the richness of shrubs and herbaceous plants would increase and would be higher under RCP 4.5. On the other hand, under RCP 4.5, the Shannon index increased slightly, while under RCP 8.5 the index was lower at lower altitudes and remained more or less stable at higher altitudes.

The Shannon vertical index and the Shannon index produced similar predictions for “diversity of tree dimensions”, i.e. the diversity of tree dimensions would increase slightly under RCP 4.5, but would decrease at lower altitudes and remain more or less stable at higher altitudes under RCP 8.5. However, considering the other two variables, the diameter differentiation would increase for the higher areas under RCP 4.5 while it would remain stable under RCP 8.5, and would decrease at the other elevations. On the other hand, there would be a general increase in height differentiation at higher elevations, with less differentiation at lower elevations.

Regarding “stand density and average tree size”, dominant height would increase in the same way in both scenarios. Similarly, stocking level would also increase in both scenarios and would be higher under RCP 8.5. Finally, the basal area of standing deadwood would remain the same under RCP 4.5, increasing at low elevations under RCP 8.5 (Figure 4).

4. Discussion

4.1. Structure of the stands

According to our results, the beech forests analyzed in this study were mainly monospecific, with very low richness of accompanying vegetation and a clear spatial separation of tree species. Around two thirds of the plots had a clustered spatial arrangement of trees, while the remaining third had a regular distribution, with random distribution occurring in a minority of cases. The stand variability was generally high in terms of density and tree size, but there was very little variability in either diameter or height in the vast majority of plots (higher for diameter). All plots were classified as fully-stocked or overstocked, which has resulted in low levels of light below-canopy, because there were at least two canopy strata in all plots. Finally, standing deadwood was observed in only a quarter of the plots.

In the words of Meyer et al. (2003), mixed stands are not a "natural feature" of beech forests, and until now, most studies have considered these forests to be monospecific (e.g. Pommerening, 2002; Bílek et al., 2011; Lombardi et al., 2012; Petritan et al., 2012). Beech forests possess several characteristics that discourage the presence of other species, including *i*) very low availability of understory light as a consequence of the crown distribution and the spatial arrangement of beech leaves (which together suppress the occurrence of light-demanding understory species, restricting them to canopy gaps) (e.g. Collet et al., 2001; Schröter et al., 2012; Hrivnák et al., 2014), and *ii*) the accumulation of a thick leaf litter layer on the soil surface (which forms a physical barrier inhibiting germination and emergence) (e.g. Mölder et al., 2008). Hence, the few plant species that withstand these particular conditions are concentrated in the gaps (e.g. Degen et al., 2005), as indicated by the values of the segregation index and shrub and herbaceous species richness.

Regarding the spatial tree distribution, clustered arrangements have been related to the possible origin of coppice stands (e.g. Campetella et al., 2016), the effect of former cattle grazing (Vera, 2000) and the typical spatial pattern of beech regeneration under parent trees or in canopy openings (e.g. Nagel et al., 2006). On the other hand, regular spacing is often the result of competition between neighbouring trees and is associated with more advanced forest states (Gadow et al., 2011). Studies using the aggregation index have reported similar results for unmanaged beech forests (e.g. Bílek et al., 2011).

However, a predominantly random distribution has been identified in almost all stands in studies using the contagion index (e.g. von Oheimb et al., 2005; Lombardi et al., 2012; Petritan et al., 2012). Several authors have demonstrated differences between the values of the aggregation and contagion indices for the same stand due to the different algorithms used (e.g. Neumann and Starlinger, 2001; Pommerening, 2002), and some authors prefer to use the aggregation index (e.g. Gleichmar and Gerold, 1998). Although this issue is beyond the scope of this paper, we found that the aggregation index provided more accurate information about the spatial distribution of trees.

Diameter and height differentiation processes are theoretically driven exclusively by natural competition and age-related dieback of mature individuals (e.g. Gadow et al., 2011). According to Bílek et al. (2011), higher heterogeneity is typical of young forests. Our results showed that the dimensions were relatively homogeneous, indicating the relative maturity of the trees. However, the absence of monostratum beech forests has been reported in other studies (e.g. Paffetti et al., 2012), demonstrating the typical bearing of beech trees growing in environments where there is competition for light (e.g. Bílek et al., 2011). Our results for the average leaf area index and luminosity are within the range of values reported in other studies (e.g. Bartelink, 1997; Meier and Leuschner, 2008).

Finally, similar results have been obtained for standing deadwood in other unmanaged beech forests (e.g. Heiri et al., 2009). However, our inventory of deadwood only considered standing dead trees, and we did not include any information about fallen trees (logs) or woody debris. We recognize this as a weakness of our study as it precludes comparison with other studies in which logs were measured, because logs contribute more to the total deadwood than standing dead trees in unmanaged forests (Christensen et al., 2005).

The results obtained in terms of the correlation between indices showed that regular stands are less dense than clustered stands and have taller and thicker trees, which may indicate that the stands are older (Wijdeven, 2004). A shift from an aggregated distribution of new recruits through a random to a regular distribution in large trees is a natural trend derived from direct density-dependent competition between neighbouring individuals, i.e. young beech forests start off being clumped and gradually become more uniform (Wolf, 2005). On the other hand, a higher stocking level indicates unmanaged forests (Schütz et al., 2016), which implies more competition and consequently higher mortality (e.g.

Neumann and Starlinger, 2001; Condés et al., 2013). The presence of other tree species increases the vertical distribution and canopy heterogeneity in beech stands (Petritan et al., 2012; Hrivnák et al., 2014), which favours light transmission to the understory (Barbier et al., 2008) and therefore increases the understory species richness (e.g. Mölder et al., 2008).

4.2. Environmental patterns

Regarding “spatial tree distribution” indices, the aggregation index was related to lithostratigraphy and texture (see Table 6). According to the lithostratigraphy, the regular tree distribution is associated with igneous and metamorphic rocks. However, clustered arrangements do occur in sedimentary soils. Even after conducting a thorough literature review, we could not clearly establish the reasons for the previous relationship.

Regarding “plant richness and species diversity”, RF only retained isothermality as an independent variable for tree richness, while for shrub and herbaceous richness and the Shannon index, a set of edaphic and thermal variables proved significant (see Table 6). In terms of thermal variables, our findings show that higher temperatures (mean, maximum of the warmest month, etc.) and less variable temperatures (seasonality and annual range) are associated with greater tree and understory species diversity (Figures S1). These results are consistent with the fact that mixed stands occur naturally in sites where the combination of drought and warmth restricts the competitiveness of beech (e.g. Pretzsch et al., 2013) and that the greater diversity in the tree stratum affects the accompanying vegetation (e.g. Mölder et al., 2008). Indeed, beech is more resistant to drought in mixed stands than in monospecific stands (Pardos et al., 2021).

From an edaphological perspective, the soil pH may be explained by the monospecificity of the stands under study. Soil pH is lower in pure beech stands than in mixed stands as beech litter is more acidic than the other species identified in the study plots (e.g. Guckland et al., 2009), and litter pH affects soil pH (Marcos et al., 2010). Therefore, a higher pH implies higher tree richness, which favours light transmission to the understory and increases the understory species richness, as previously stated. On the other hand, the forest overstory composition affects the chemical, physical and biological characteristics of soil (Augusto et al., 2002), because it involves differences in soil development (e.g. Kooch et al., 2012). A higher sand content is associated with better soil aeration (Brandl et al., 2014), and several authors have used this parameter to predict the presence of tree species such as beech (e.g. Piedallu et al., 2016). However, we have not found any study that has determined the reason for the relationship between stand diversity and sand content of the soil. Finally, our findings show that higher contents of nitrogen and potassium in soil are associated with more diverse stands (Figures S1). According to Talkner et al. (2009) and (2010), both of these elements occur at higher concentrations in mixed stands than in beech-dominated stands due to deposition and canopy exchange.

Regarding “diversity of tree dimensions and vertical structure”, climatic variables were relatively more important in diameter differentiation and the Shannon vertical index, while edaphic variables were more important in relation to height differentiation. Precipitation and temperature are known to be closely related to radial growth in beech forests (e.g. Maxime and Hendrik, 2011; Van der Maaten, 2012) and soil parent material and soil water holding capacity mainly affect height growth (e.g. Hill et al., 1948; Carmean, 1954). However, the direct relationships between climate and soil and diameter and height differentiations have not yet been addressed.

Regarding “stand density and average tree size”, stocking level was mainly determined by edaphic variables followed by climatic and terrain variables), while dominant height was mainly related to climatic variables (terrain and soil variables) (see Table 6). According to Seynave et al. (2008), soil parameters explain approximately 30% of the variation in potential beech forest growth. For instance, bulk density, a physical soil property intrinsically related to other physical and chemical variables, is a proxy for sand content, soil organic matter and nutrient availability (e.g. Sakin, 2012; Chaudhari et al., 2013). Bulk density therefore affects soil aeration, solute transport and storage as well as the outcome of soil C stocks (Nemes et al., 2010). Fresh, well-aerated fertile soils, with good water retention capacity, favour the development and growth of beech forests (e.g. Brandl et al., 2014), as does a higher organic matter content, which implies higher concentrations of phosphorus, nitrogen and carbon (Talkner et al., 2009; 2010). Nitrogen and phosphorus are the most frequently limiting macronutrients for primary production in beech forests (Vitousek et al., 2010). In terms of climatic variables, temperature is again more important than precipitation, as a result of the conditions of humidity to which these forests are subjected in the study area. On the other hand, the wetness index shows that beech is very sensitive to excess water, as previously stated. The other significant variables have already been discussed.

Regarding dominant height, several studies have shown that low winter temperatures and high summer temperatures negatively affect height growth in beech (e.g. Scharnweber et al., 2011; Hacket-Pain et al., 2016). Our findings are consistent with previous findings suggesting that beech grows optimally within a certain temperature range, so that growth of the trees is negatively affected by extreme temperatures outside of that range. Topographic position, exposure and slope also significantly affect forests. Our findings show that a steeper slope implies higher dominant height (Table 6 and Figures S1). This is because dominant trees consume many more of the available resources than their smaller neighbours on steep slopes, assuming higher growth rates of dominant trees (Pretzsch and Dieler, 2011).

Finally, regarding "standing deadwood", the mean diurnal range of temperatures significantly affected the basal area of the standing dead trees (Table 6), indicating that greater standing dead wood is associated with greater mean diurnal range (Figure S1). This may be due to the fact that high daily maximum temperature and the vapour pressure deficit induce stress during the warmest and driest time of the day, limiting growth and potentially resulting in death of the trees (Thom et al., 2020).

4.3. Forecasting the effects of climate change on the beech forest structure

Understanding how vegetation dynamics are impacted by climate is a key challenge in a world undergoing anthropogenic climate change. Our findings indicate that climate change will affect most structural features of forests, except the diversity of tree positions, which is mainly driven by soil factors. The intensity of the effects depends on the particular feature and the climate change scenario considered.

Previous studies have predicted a drastic reduction in suitable habitat area for beech forests in the Cantabrian Range (e.g. Kramer et al., 2010; Castaño-Santamaría et al., 2019), which would result in a deterioration of growth conditions, as a consequence of climate change. In particular, a latitudinal shift towards the north and an upwards elevational shift are foreseen. Our predictions clearly show the effect of elevation on temperatures and precipitation, with effects related to a worsening of suitable conditions for beech at lower altitudes. However, at higher elevations beech forests are less sensitive to drought and heat stress (see Psidova et al., 2018). Nonetheless, the less favourable conditions may indicate that beech would lose its fundamental competitive advantage over other species, which could result in a loss of dominance, higher mortality or lower regeneration (Leuschner, 1998; Allen et al., 2010; Silva et al., 2012). As a consequence, the appearance of other species would reduce the monospecificity of the stands and increase their dimensional diversity (e.g. Pretzsch et al., 2013). In fact, beech is currently being replaced in NE Spain by species that are better adapted to cope with the warmer and drier conditions (e.g. holm oak and European holly) (see Peñuelas et al., 2007), which implies an increase in tree richness relative to pure beech forests. Thus, the present findings appear to be consistent with all of these previous findings.

Nevertheless, according to Gray and Hamann (2013), projections regarding climate change should not be interpreted literally as predicted species demographics, and negative projections do not necessarily entail the removal of current populations (Hampe, 2004). For instance, the tallest and thickest beech trees will probably persist (e.g. Charru et al., 2017), and the microclimatic buffering capacity of beech forest canopies may partly offset the impact of global climate change on subcanopy processes (Thom et al., 2020). In fact, our findings suggest that the tallest and thickest beech trees would persist, which would lead to an increase in the basal area and the dominant and average heights of beech trees. However, there is also no clear pattern in these increases (see Albert and Schmidt, 2010; Brandl et al., 2018 or Nothdurft et al., 2012 as examples). It is evident that, although information about the responses of forest ecosystems to climate change has increasingly been reported in recent years, some uncertainties remain.

5. Conclusions

Beech-dominated forests in the Cantabrian Range are mostly monospecific, overstocked and never monostratified, with very closed canopies and low levels of light below the canopy. These forests exhibit a moderately clustered spatial arrangement when young becoming more regular as they mature, with a clear spatial separation of tree species and high overall variability in density and tree size. Nevertheless, there is a scarce diameter and height differentiation in the vast majority of plots (greater for diameter), and only one quarter of the stands have standing deadwood.

Although the findings must be considered with caution, as the predictors retained by models are to some extent determined by the algorithm used, we found that tree spatial distribution is only driven by soil factors, whereas tree species richness, vertical structure and basal area of standing dead trees are driven exclusively by climatic variables, and they are therefore very sensitive to climate change. The remaining structural features are driven by a mixture of types of factors. Shrub and herbaceous species richness and tree diameter differentiation are explained in similar ways by soil and climatic variables, while dominant height is mainly driven by climatic variables and, by contrast, tree species intermingling, tree height differentiation and stocking level are mainly driven by soil-related variables.

The climatic conditions forecast for the study area will lead to deterioration of suitable conditions for beech (mainly at lower altitudes), implying a reduction in tree richness and diversity of tree dimensions but an increase in stocking level and standing deadwood (more canopy gaps) and consequently increased richness of shrubs and herbaceous species. Changes in climatic conditions will be less marked at higher elevations, coinciding with the upwards elevational shift predicted as a consequence of global warming. In this zone, tree species diversity would be slightly higher under the moderate climate change scenario, but would remain more or less stable under the pessimistic scenario.

In summary, our findings indicate that beech will lose its fundamental competitive advantage over other species, which may result in a shift to more resilient mixed stands. These predictions may be useful for helping decision-makers to develop plans for protecting biodiversity, forest management and species re-habitation plans to prevent or mitigate the impact of climate change on beech forests.

740

6. Acknowledgements

While undertaking the present study, the first author was in receipt of a Severo Ochoa Fellowship from the Asturias Government (code 09/111). The authors are grateful to the Asturias and Castilla y León Government Forest and Environmental Services for forest access and inventory permissions granted. Our thanks to SERIDA for lending us the Nikon FC-E9 fish-eye lens. The authors thank Dr Juan Luis Fernández Martínez and Dr José Javier Corral Rivas for their invaluable help during statistical analysis and structural data processing, respectively. The authors also thank Dr María Castaño Díaz and forestry colleagues Mr José Manuel Álvarez González, Mr Jesús Aladro Aladro and Mr Pablo González Vallina for invaluable help during field sampling. Finally, the authors thank two anonymous referees for their valuable, highly constructive comments and suggestions on a previous version of the manuscript.

7. References

Albert, M., Schmidt, M., 2010. Climate-sensitive modelling of site-productivity relation- ships for Norway spruce (*Picea abies* (L.) Karst.) and common beech (*Fagus sylvatica* L.). For. Ecol. Manage. 259, 739–749. https://doi.org/10.1016/j.foreco.2009.04.039.

Allen, C.D., Macalady, A.K., Chenchouni, H., Bachelet, D., McDowell, N., Vennetier, M., Kitzberger, T., Rigling, A., Breshears, D.D., Hogg, E.H., González, P., Fensham, R., Zhang, Z., Castro, J., Demidova, N., Lim, J.H., Allard, G., Running, S.W., r, Semerci, A., Cobb, N., 2010. A global overview of drought and heat-induced tree mortality reveals emerging climate change risks for forests. For. Ecol. Manage. 259 (4), 660-684. https://doi.org/10.1016/j.foreco.2009.09.001.

Augusto, L., Ranger, J., Binkley, D., Rothe, A., 2002. Impact of several common tree species of European temperate forests on soil fertility. Ann. For. Sci. 59, 233-253. https://doi.org/10.1051/forest:2002020.

Ballabio, C., Lugato, E., Fernández-Ugalde, O., Orgiazzi, A., Jones, A., Borrelli, P., Montanarella, L. and Panagos, P., 2019. Mapping LUCAS topsoil chemical properties at European scale using Gaussian process regression. Geoderma, 355: 113912. https://doi.org/10.1016/j. geoderma.2019.113912.

Barbier, S., Gosselin, F., Belandier, P., 2008. Influence of tree species on understorey vegetation diversity and mechanisms involved – A critical review for temperate and boreal forests. For. Ecol. Manage. 254, 1-15. https://doi.org/10.1016/j.foreco.2007.09.038.

Bartelink, H.H., 1997. Allometric relationships for biomass and leaf area of beech (*Fagus sylvatica* L.). Ann. Sci. For. 54, 39-50. https://doi.org/10.1051/forest:19970104.

Becking, J.H., 1953. Einige Gesichtspunkte für die Durchführung von vergleichenden Durchforstungsversuchen in gleichaltrigen Beständen. In: Proc. 11th Congress IUFRO. Rome, pp. 580-582.

Bílek, L., Remeš, J., Zahradnik, D., 2011. Managed vs. unmanaged. Structure of beech forest stands (*Fagus sylvatica* L.) after 50 years of development, Central Bohemia. Forest Syst. 20 (1), 122-138. https://doi.org/10.5424/fs/2011201-10243.

Bonferroni, C.E., 1936. Teoria statistica delle classi e calcolo delle probabilità. Pubblicazioni del R Istituto Superiore di Scienze Economiche e Commerciali di Firenze 8, 3-62.

Brandl, S., Falk, W., Klemmt, H.J., Stricker, G., Bender, A., Rötzer, T., Pretzsch, H., 2014. Possibilities and limitations of spatially explicit site index modelling for spruce based on national forest inventory data and digital maps of soil and climate in Bavaria (SE Germany). Forests 5 (11), 2626-2646. https://doi.org/10.3390/f5112626.

Brandl, S., Mette, T., Falk, W., Vallet, P., Rötzer, T., Pretzsch, H., 2018. Static site indices from different national forest inventories: harmonization and prediction from site conditions. Ann. For. Sci. 75, 56. https://doi.org/10.1007/s13595-018-0737-3.

Breiman, L., 2001. Random forests. Mach. Learn. 45 (1), 5-32. https://doi.org/10.1023/A:1010933404324.

Burkhart, H. E., Tomé, M., 2012. Modeling Forest Trees and Stands. Springer.

Campetella, G., Canullo, R., Gimona, A., Garadnai, J., Chiarucci, A., Giorgini, D., Angelini, E., Cervellini, M., Chelli, S., Bartha, S., 2016. Scale-dependent effects of coppicing on the species pool of late successional beech forests in the central Apennines, Italy. Appl. Veg. Sci. 19 (3), 474-485. https://doi.org/10.1111/avsc.12235.

Carmean, W.H., 1954. Site quality for Douglas-fir in south-western Washington and its relationship to precipitation, elevation, and physical soil properties. Soil Sci. Soc. Am. Proc. 18, 330-334.

Castaño-Santamaría, J., López-Sánchez, C.A., Obeso, J.R., Barrio-Anta, M., 2019. Modelling and mapping beech forest distribution and site productivity under different climate change scenarios in the Cantabrian Range (North-western Spain). For. Ecol. Manage. 450, 117488. https://doi.org/10.1016/j.foreco.2019.117488.

Chaudhari, P.R., Ahire, D.V., Ahire, V.D., Chkravarty, M., Maity, S., 2013. Soil bulk density as related to soil texture, organic matter content and available total nutrients of Coimbatore soil. Int. J. Sci. Res. 3(2), 1-8.

Charru, M., Seynave, I., Hervé, J.C., Bertrand, R., Bontemps, J.D., 2017. Recent growth changes in Western European forests are driven by climate warming and structured across tree species climatic habitats. Ann. For. Sci. 74, 33. https://doi.org/10.1007/s13595-017-0626-1.

Choudhury, P., Allen, R.T., Endres, M.G., 2021. Machine learning for pattern discovery in management research. Strat. Mgmt. J. 42, 30-57. https://doi.org/10.1002/smj.3215.

Christensen, M., Hahn, K., Mountford, E.P., Odor, P., Standovár, T., Rozenbergar, D., Diaci, J., Wijdeven, S., Meyer, P., Winter, S., Vrska, T., 2005. Dead wood in European beech (*Fagus sylvatica*) forest reserves. For. Ecol. Manage. 210, 267-282. https://doi.org/10.1016/j.foreco.2005.02.032.

Clark, P.J., Evans, F.C., 1954. Distance to nearest neighbour as a measure of spatial relationships in populations. Ecology 35, 445-453.

Collet, C., Lanter, O., Pardos, M., 2001. Effects of canopy opening on height and diameter growth in naturally regenerated beech seedlings. Ann. For. Sci. 58 (2), 127-134. https://doi.org/10.1051/forest:2001112.

Condés, S., del Río, M., Sterba, H., 2013. Mixing effect on volume growth of *Fagus sylvatica* and *Pinus sylvestris* is modulated by stand density. For. Ecol. Manage. 292, 86-95. https://doi.org/10.1016/j.foreco.2012.12.013.

Condés, S., Vallet, P., Bielak, K., Bravo-Oviedo, A., Coll, L.L., Ducey, M.J., Pach, M., Pretzsch, H., Sterba, H., Vayreda, J., del Río, M., 2017. Climate influences on the maximum size-density relationship in Scots pine (*Pinus sylvestris* L.) and European beech (*Fagus sylvatica* L.) stands. For. Ecol. Manage. 385, 295-307. https://doi.org/10.1016/j.foreco.2016.10.059.

Corral-Rivas, J.J. 2006. Models of tree growth and spatial structure for multi-species uneven-aged forests in Durango (Mexico). PhD Thesis. Georg-August-Universität Göttingen. 135 pp.

Davies, O., Pommerening, A., 2008. The contribution of structural indices to the modelling of Sitka spruce (*Picea sitchensis*) and birch (*Betula* spp.) crowns. For. Ecol. Manage. 256, 68-77. https://doi.org/10.1016/j.foreco.2008.03.052.

Degen, T., Devillez, F., Jacquemart, A.L., 2005. Gaps promote plant diversity in beech forests (*Luzulo-Fagetum*), North Vosges, France. Ann. For. Sci. 62, 429–440. https://doi.org/10.1051/forest:2005039.

Díaz, T.E., Fernández, J.A., 1987. Asturias y Cantabria, in: Peinado Lorca, M., Rivas-Martínez, S. (Eds.), La vegetación de España. Servicio de publicaciones de la Universidad de Alcalá de Henares, Madrid, pp. 77-116.

Falk, W., Hempelmann, N., 2013. Species favourability shift in Europe due to climate change: A case study for *Fagus sylvatica* L. and *Picea abies* (L.) Karst. based on an ensemble of climate models. J. Climatol. 2013, 1–18. https://doi.org/10.1155/2013/ 787250.

Fang, J., Lechowicz, M.J., 2006. Climatic limits for the present distribution of beech (*Fagus* L.) species in the world. J. Biogeogr. 33, 1804–1819. https://doi.org/10.1111/ j.1365-2699.2006.01533.x.

Franklin, J.F., Cromack, K.J., Denison, W., McKee, A., Maser, C., Sedell, J., Swanson, F., Juday, G., 1981. Ecological Characteristics of Old-Growth Douglas-Fir Forests. USDA Forest Service General Technical Report PNW-118, 48 pp.

Frazer, G.W., Canham, C.D., Lertzman, K.P., 1999. Gap Light Analyser (GLA), version 2.0: imaging software to extract canopy structure and gap light indices from true-colour fisheye photographs. Simon Fraser University, Burnaby, BC, and the Institute of Ecosystem Studies, Millbrook, NY.

Füldner, K., 1995. Strukturbeschreibung von Buchen-Edellaubholz-Mischwäldern. PhD Thesis. Göttingen University. Cuvillier Verlag, Göttingen.

Gadow, K.v., 1993. Zur Bestandesbeschreibung in der Forsteinrichtung. Forst und Holz 48, 601-606.

Gadow, K.v., 1999. Waldstruktur und Diversität. Allg. Forst- u J. –Ztg. 170, 117-122.

Gadow, K.v., Hui, G.Y., Albert, M., 1998. Das Winkelmaβ-ein Strukturparameter zur Beschreibung der Individualverteilung in Waldbeständen. Centralbl. ges. Forstwesen 115, 1-10.

Gadow, K.v., Zhang, C.Y., Wehenkel, C., Pommerening, A., Corral-Rivas, J., Korol, M., Myklush, S., Hui, G.Y., Kiviste, A., Zhao, X.H., 2011. Forest Structure and Diversity, in: Pukkala, T., Gadow, K. v. (Eds.) Continuous Cover Forestry. Springer, Dordrecht. pp 29-83.

García, D., Quevedo, M., Obeso, J.R., Abajo, A., 2005. Fragmentation patterns and protection of montane forest in the Cantabrian range (NW Spain). For. Ecol. Manage. 208, 29-43. https://doi.org/10.1016/j.foreco.2004.10.071.

Gleichmar, W., Gerold, D., 1998. Indizes zur Charakterisierung der horizontalen Baumverteilung. Forstwiss. Centralbl. 117, 69-80. https://doi.org/10.1007/BF02832960.

Gray, L.K., Hamann, A., 2013. Tracking suitable habitat for tree populations under climate change in western North America. Climatic Change 117, 289-303. https://doi.org/10.1007/s10584-012-0548-8.

Guckland, A., Jacob, M., Flessa, H., Thomas, F.M., Leuschner, C., 2009. Acidity, nutrient stocks, and organic-matter content in soils of a temperate deciduous forest with different abundance of European beech (*Fagus sylvatica* L.). J. Plant Nutr. Soil Sci. 172, 500-511. https://doi.org/10.1002/jpln.200800072.

Hacket-Pain, A.J., Cavin, L., Friend, A.D., Jump, A.S., 2016. Consistent limitation of growth by high temperature and low precipitation from range core to southern edge of European beech indicates widespread vulnerability to changing climate. Eur. J. For. Res. 135, 897–909. https://doi.org/10.1007/s10342-016-0982-7.

Hale, S.E., Edwards, C., 2002. Comparison of film and digital hemispherical photography across a wide range of canopy densities. Agric. For. Meteorol. 112, 51-56. https://doi.org /10.1016/S0168-1923(02)00042-4.

Hall, M., Frank, E., Holmes, G., Pfahringer, B., Reutemann, P., Witten, I.H., 2009. The WEKA data mining software: An update. SIGKDD Explorations 11 (1), 10-18. https://doi.org/10.1145/1656274.1656278.

Hampe, A., 2004. Bioclimate envelope models: what they detect and what they hide. Glob. Ecol. Biogeogr. 12 (5), 469-471. https://doi.org/10.1111/j.1466-822X.2004.00090.x.

Harmon, M.E., Franklin, J.F., Swanson, F., Sollins, P., Gregory, S.V., Lattin, J.D., Anderson, N.H., Cline, S.P., Aumen, N.G., Sedell, J.R., Lienkaemper, G.W., Cromack, J., Cummins, K.W., 1986. Ecology of coarse woody debris in temperate ecosystems. Adv. Ecol. Res. 15, 133–302.

Harris, R.M.B., Grose, M.R., Lee, G., Bindoff, N.L., Porfirio, L.L., Fox-Hughes, P., 2014. Climate projections for ecologists. Wiley Interdiscip. Rev. Clim. Change 5, 621–637. https://doi.org/10.1002/wcc.291.

Hart, H.M.J., 1928. Stamtal en Dunning. Proefstation Boschwesen, Batavia, Mededelingen. 21.

Heiri, C., Wolf, A., Rohrer, L., Bugmann, H., 2009. Forty years of natural dynamics in Swiss beech forests: structure, composition, and the influence of former management. Ecol. Appl. 19 (7), 1920-1934. https://doi.org/10.1890/08-0516.1.

Hengl, T., Mendes de Jesus, J., Heuvelink, G.B.M., Ruiperez Gonzalez, M., Kilibarda, M., Blagotic, A., Shangguan, W., Wright, M.N., Geng, X., Bauer-Marschallinger, B., Guevara, M.A., Vargas, R., MacMillan, R.A., Batjes, N.H., Leenars, J.G.B., Ribeiro, E., Wheeler, I., Mantel, S., Kempen, B., 2017. SoilGrids250m: global gridded soil information based on machine learning. PloS ONE 12 (2), e0169748. https://doi.org/10.1371/journal.pone.0169748.

Hijmans, R.J., Cameron, S.E., Parra, J.L., Jones, P., Jarvis, A., 2005. Very high resolution interpolated climate surfaces for global land areas. Int. J. Climatol. 25, 1965-1978. https://doi.org/10.1002/joc.1276.

Hill, W.W., Arnst, A., Bond, R.M., 1948. Method of correlating Douglas-fir to site quality. J. Forest. 46, 835-841.

Hrivnák, R., Gömöry, D., Slezák, M., Ujházy, K., Hédl, R., Jarčuška, B., Ujházyová, M., 2014. Species Richness Pattern along Altitudinal Gradient in Central European Beech Forests. Folia Geobot. 49, 425-441. https://doi.org/10.1007/s12224-013-9174-0.

Hui, G.Y., Albert, M., Gadow, K.v., 1998. Das Umgebungsmab als Parameter zur Nachbildung von Bestandesstrukturen. Forstwiss. Centbl. 117, 258-266.

Hui, G.Y., Gadow, K. v. 2002. Das Winkelmass – Herleitung des optimalen Standardwinkels. Allg. Forst- u J. –Ztg. 173, 173-177.

IGME, 2015a. Mapa Geológico de España a escala 1:200.000. Instituto Geológico y Minero de España, Ministerio de Ciencia, Innovación y Universidades. Madrid.

IGME, 2015b. Mapa Geológico de la Península Ibérica, Baleares y Canarias a escala 1:1.000.000. Instituto Geológico y Minero de España, Ministerio de Ciencia, Innovación y Universidades. Madrid.

IPCC, 2013. Climate Change 2013: The physical science basis. Contribution of working group I to the fifth assessment report of the Intergovernmental Panel of Climate Change. Cambridge University Press. Cambridge, New York.

Jonckheere, I., Fleck, S., Nackaerts, K., Muys, B., Coppin, P., Weiss, M., Baret, F., 2004. Review of methods for in situ leaf area index determination Part I. Theories, sensors and hemispherical photography. Agric. For. Meteorol. 121, 19-35. https:// doi.org/10.1016/j.agrformet.2003.08.027.

Kooch, Y., Hosseini, S.M., Zaccone, C., Jalilvand, H., Hojjati, S.M., 2012. Soil organic carbon sequestration as affected by afforestation: the Darab Kola forest (North of Iran) case study. J. Environ. Monit. 14, 2438-2446. https://doi.org/10.1039/c2em30410d.

Kramer, K., Degen, B., Buschbom, J., Hickler, T., Thuiller, W., Sykes, M.T., de Winter, W., 2010. Modelling exploration of the future of European beech (*Fagus sylvatica* L.) under climate change- Range, abundance, genetic diversity and adaptive response. For. Ecol. Manage. 259, 2213-2222. https://doi.org/10.1016/j.foreco.2009.12.023.

Leuschner, C., 1998. Mechanismen der Konkurrenzüberlegenheit der Rotbuche. Berichte der Reinh.-Tüxen-Gesellschaft 10, 5-18.

Liu, Z., Peng, C., Work, T., Candau, J.N., DesRochers, A., Kneeshaw, D., 2018. Application of machine-learning methods in forest ecology: recent progress and future challenges. Environ. Rev. 26, 339-350. https://doi.org/10.1139/er-2018-0034.

Lombardi, F., Klopcic, M., Di Martino, P., Tognetti, R., Chirici, G., Boncina, A., Marchetti, M., 2012. Comparison of forest stand structure and management of silver fir– European beech forests in the Central Apennines, Italy and in the Dinaric Mountains, Slovenia. Plant Biosyst. 146 (1), 114-123. https://doi.org/10.1080/11263504.2011.623190.

Long, J.N., 1985. A practical approach to density management. For. Chron. 61, 23-27.

Marcos, E., Calvo, L., Marcos, J.A., Taboada, A., Tárrega, R., 2010. Tree effects on the chemical topsoil features of oak, beech and pine forests. Eur. J. For. Res. 129, 25-30. https://doi.org/10.1007/s10342-008-0248-0.

Mason, E.G., Diepstraten, M., Pinjuv, G.L., Lasserre, J.P., 2012. Comparison of direct and indirect leaf area index measurements of *Pinus radiata* D. Don. Agric. For. Meteorol. 166-167, 113-119. https://doi.org/10.1080/02827588909382582.

Maxime, C., Hendrik, D., 2011. Effects of climate on diameter growth of co-occurring *Fagus sylvatica* and *Abies alba* along an altitudinal gradient. Trees 25, 265-276. https://doi.org/10.1007/s00468-010-0503-0.

Meier, I.C., Leuschner, C., 2008. Leaf size and leaf area index in *Fagus sylvatica* forests: competing effects of precipitation, temperature, and nitrogen availability. Ecosystems 11, 655-669. https://doi.org/10.1007/s10021-008-9135-2.

Meyer, P., Tabaku, V., Lüpke, B.v., 2003. Die Struktur albanischer Rotbuchen-Urwälder-Ableitungen für eine naturnahe Buchenwirtschaft. Forstwiss. Centralbl. 122, 47-58. https://doi.org/10.1046/j.1439-0337.2003.02041.x.

Mölder, A., Bernhardt-Römermann, M., Schmidt, W., 2008. Herb-layer diversity in deciduous forests: Raised by tree richness or beaten by beech? For. Ecol. Manage. 256, 272-281. https://doi.org/10.1016/j.foreco.2008.04.012.

Montgomery, R.A., Chazdon, R.L., 2001. Forest structure, canopy architecture, and light transmittance in old-growth and second-growth tropical rain forests. Ecology 82, 2707–2718. https://doi.org/10.2307/2679955.

Nagel T.A., Svoboda M., Diaci, J., 2006. Regeneration patterns after intermediate wind disturbance in an old-growth *Fagus–Abies* forest in southeastern Slovenia. For. Ecol. Manage. 226, 268-278. https://doi.org/10.1016/j.foreco.2006.01.039.

Nemes, A., Quebedeaux, B., Timlin, D.J., 2010. Ensemble Approach to Provide Uncertainty Estimates of Soil Bulk Density. Soil Sci. Soc. Am. J. 74, 1938-1945. https://doi.org/10.2136/sssaj2009.0370.

Neumann, M., Starlinger, F., 2001. The significance of different indices for stand structure and diversity in forests. For. Ecol. Manage. 145, 91-106. https://doi.org/10.1016/s0378-1127(00)00577-6.

Nothdurft, A., Wolf, T., Ringeler, A., Bohner, J., Saborowski, J., 2012. Spatio-temporal prediction of site index based on forest inventories and climate change scenarios. For. Ecol. Manage. 279, 97–111. https://doi.org/10.1016/j.foreco.2012.05.018.

Paffetti, D., Travaglini, D., Buonamici, A., Nocentini, S., Vendramin, G.G., Giannini, R., Vettori, C., 2012. The influence of forest management on beech (*Fagus sylvatica* L.) stand structure and genetic diversity. For. Ecol. Manage. 284, 34-44. https://doi.org/10.1016/j.foreco.2012.07.026.

Pardos, M., del Río, M., Pretzsch, H., Jactel, H., Bielak, H., Bravo, F., Brazaitis, G., Defossez, E., Engel, M., Godvod, K., Jacobs, K., Jansone, L., Jansons, A., Morin, X., Nothdurft, A., Oreti, L., Ponette, Q., Pach, M., Riofrío, J., Ruíz-Peinado, R., Tomao, A., Uhl, E., Calama, R., 2021. The greater resilience of mixed forests to drought mainly depends on their composition: Analysis along a climate gradient across Europe. For. Ecol. Manage. 481, 118687. https://doi.org/10.1016/j.foreco.2020.118687.

Peñuelas, J., Ogaya, R., Boada, M., Jump, A.S., 2007. Migration, invasion and decline: changes in recruitment and forest structure in a warming-linked shift of European beech forest in Catalonia (NE Spain). Ecography 30, 829-837. https://doi.org/10.1111/j.2007.0906-7590.05247.x.

Petritan, A.M., Biris, I.A., Merce, O., Turcu, D.O., Petritan, I.C., 2012. Structure and diversity of a natural temperate sessile oak (*Quercus petraea* L.) – European Beech (*Fagus sylvatica* L.) forest. For. Ecol. Manage. 280, 140-149. https://doi.org/10.1016/j.foreco.2012.06.007.

Piedallu, C., Gégout, J.C., Lebourgeois, F., Seynave, I., 2016. Soil aeration, water deficit, nitrogen availability: acidity and temperature all contribute to shaping tree species distribution in temperate forests. J. Veg. Sci. 27, 387-399. https://doi.org/10.1111/jvs.12370.

Pielou, E.C., 1977. Mathematical Ecology. John Wiley & Sons.

Pommerening, A., 2002. Approaches to quantifying forest structures. Forestry 75, 305-324. https://doi.org/10.1093/forestry/75.3.305.

Pommerening, A., 2006. Evaluating structural indices by reversing forest structural analysis. For. Ecol. Manage. 224, 266-277. https://doi.org/10.1016/j.foreco.2005.12.039.

Pommerening, A., 2007. Concepts of Measuring and Reconstructing Spatial Woodland Structure, in: Newton, P.F., LeMay, V.M. (Eds.). Complex Stand Structures and Associated Dynamics: Measurement Indices and Modelling Approaches. Ontario Forest Research Institute. Forest Research Information Paper, nº 167. Ontario Ministry of Natural Resources. Sault Ste. Marie, Ontario, Canadá. pp. 36-37.

Pommerening, A., Stoyan, D., 2006. Edge-correction needs in estimating indices of spatial forest structure. Can. J. For. Res. 36, 1723-1739. https://doi.org/10.1139/X06-060.

Pommerening, A., LeMay, V., Stoyan, D., 2011. Model-based analysis of the influence of ecological processes on forest point pattern formation-A case study. Ecol. Modell. 222, 666-678. https://doi.org/10.1016/j.ecolmodel.2010.10.019.

Pretzsch, H., 1996. Strukturvielfalt als Ergebnis waldbaulichen Handelns. Allg. Forst. –u. J. –Ztg. 167 (11), 213-221.

Pretzsch, H., 1997. Analysis and modelling of spatial stand structures. Methodological considerations based on mixed beech-larch stands in Lower Saxony. For. Ecol. Manage. 97, 237-253. https://doi.org/10.1016/S0378-1127(97)00069-8.

Pretzsch, H., 1998. Structural diversity as a result of silvicultural operations. Lesnictví-Forestry 44, 429-439.

Pretzsch, H., 2009. Forest dynamics, growth and yield. Springer-Verlag, Berlin.

Pretzsch, H., Dieler, J., 2011. The dependency of the size-growth relationship of Norway spruce (*Picea abies* [L.] Karst.) and European beech (*Fagus sylvatica* L.) in forest stands on long-term site conditions, drought events, and ozone stress. Trees 25, 355-369. https://doi.org/10.1007/s00468-010-0510-1.

Pretzsch, H., Schütze, G., Uhl, E., 2013. Resistance of European tree species to drought stress in mixed versus pure forests: evidence of stress release by inter-specific facilitation. Plant Biol. 15, 483-495. https://doi.org/10.1111/j.1438-8677.2012.00670.x.

Psidova, E., Zivcak, M., Stojnic, S., Orlovic, S., Gomory, D., Kucerova, J., Ditmarova, L., Strelcova, K., Brestic, M., Kalaji, H.M., 2018. Altitude of origin influences the responses of PSII photochemistry to heat waves in European beech (*Fagus sylvatica* L.). Environ. Exp. Bot. 152, 97-106. https://doi.org/10.1016/j.envexpbot.2017.12.001.

Reineke, L.H., 1933. Perfecting a stand-density index for even-aged forests. J. Agric. Res. 46, 627-638.

Riahi, K., Rao, S., Krey, V., Cho, C., Chirkov, V., Fischer, G., Kindermann, G., Nakicenovic, N., Rafaj, P., 2011. RCP 8.5-A scenario of comparatively high greenhouse gas emis- sions. Clim. Change 109, 33–57. https://doi.org/10.1007/s10584-011-0149-y.

Rich, P.M., 1990. Characterizing plant canopies with hemispherical photographs. Remote Sens. Rev. 5, 13-29.

Rubio-Cuadrado, A., Camarero, J.J., del Río, M., Sánchez-González, M., Ruiz-Peinado, R., Bravo-Oviedo, A., Gil, L., Montes, F., 2018. Long-term impacts of drought on growth and forest dynamics in a temperate beech-oak-birch forest. Agr. For. Meteorol. 259, 48-59. https://doi.org/10.1016/j.agrformet.2018.04.015.

Ruprecht, H., Dhar, A., Aigner, B., Oitzinger, G., Klumpp, R., Vacik, H., 2010. Structural diversity of English yew (*Taxus baccata* L.) populations. Eur. J. For. Res. 129, 189-198. https://doi.org/10.1007/s10342-009-0312-4.

Ryan, T.P., 1997. Modern regression methods. John Wiley & Sons, New York.

Sakin, E., 2012. Organic carbon organic matter and bulk density relationships in arid-semi arid soils in Southeast Anatolia region. Afr. J. Biotechnol. 11, 1373-1377. https://doi.org/10.5897/AJB11.2297.

Sánchez-Azofeifa, G.A., Guzmán-Quesada, J.A., Vega-Araya, M., Campos-Vargas, C., Milena Durán, S., D'Souza, N., Gianoli, T., Portillo-Quintero, C., Sharp, I. 2017. Can terrestrial laser scanners (TLSs) and hemispherical photographs predict tropical dry forest succession with liana abundance? Biogeosciences 14, 977-988. https://doi.org/10.5194/bg-14-977-2017.

SAS Institute Inc., 2004. SAS/ETS 9.1 User's Guide. SAS Institute Inc., Cary, NC, USA.

Scharnweber, T., Manthey, M., Criegee, C., Bauwe, A., Schröder, C., Wilmking, M., 2011. Drought matters — declining precipitation influences growth of *Fagus sylvatica* L. and *Quercus robur* L. in north-eastern Germany. For. Ecol. Manage. 262, 947–961. https:// doi.org/10.1016/j.foreco.2011.05.026.

Schröter, M., Härdtle, W., von Oheimb, G., 2012. Crown plasticity and neighborhood interactions of European beech (*Fagus sylvatica* L.) in an old-growth forest. Eur. J. For. Res. 131, 787-798. https://doi.org/10.1007/s10342-011-0552-y.

Schütz, J.P., Saniga, M., Diaci, J., Vrska, T., 2016. Comparing close-to-nature silviculture with processes in pristine forests: lessons from Central Europe. Ann. For. Sci. 73, 911-921. https://doi.org/10.1007/s13595-016-0579-9.

Seynave, I., Gégout, J.C., Hervé, J.C., Dhôte, J.F., 2008. Is the spatial distribution of European beech (*Fagus sylvatica* L.) limited by its potential height growth? J. Biogeogr. 35, 1851-1862. https:///doi.org/10.1111/j.1365-2699.2008.01930.x.

Shannon, C.E., Weaver, W., 1949. The Mathematical Theory of Communication. University of Illinois Press.

Silva, D.E., Rezende Mazzella, P., Legay, M., Corcket, E., Dupouey, J.L. 2012. Does natural regeneration determine the limit of European beech distribution under climatic stress? For. Ecol. Manage. 266, 263-272. https://doi.org/10.1016/j.foreco.2011.11.031.

Silva-Flores, R., Pérez-Verdín, G., Wehenkel, C., 2014. Patterns of Tree Species Diversity in Relation to Climatic Factors on the Sierra Madre Occidental, Mexico. PLoS ONE 9(8): e105034. https://doi.org/10.1371/journal.pone.0105034.

Simpson, E.H., 1949. Measurement of diversity. Nature 163, 688.

Talkner, U., Jansen, M., Beese, F.O., 2009. Soil phosphorus status and turnover in central-European beech forest ecosystems with differing tree species diversity. Eur. J. Soil Sci. 60, 338-346. https://doi.org/10.1111/j.1365-2389.2008.01117.x.

Talkner, U., Krämer, I., Hölscher, D., Beese, F.O., 2010. Deposition and canopy exchange processes in central-German beech forests differing in tree species diversity. Plant Soil 336, 405-420. https://doi.org/10.1007/s11104-010-0491-2.

Thom, D., Sommerfeld, A., Sebald, J., Hagge, J., Müller, J., Seidl, R., 2020. Effects of disturbance patterns and deadwood on the microclimate in European beech forests. Agric. For. Meteorol. 291, 108066. https://doi.org/10.1016/j.agrformet.2020.108066.

Thomson, A.M., Calvin, K.V., Smith, S.J., Kyle, G.P., Volke, A., Patel, P., Delgado-Arias, S., Bond-Lamberty, B., Wise, M.A., Clarke, L.E., Edmonds, J.A., 2011. RCP 4.5: a pathway for stabilization of radiative forcing by 2100. Clim. Change 109, 77–94. https://doi.org/10.1007/s10584-011-0151-4.

Tyrrell, L.F., Crow, T.R., 1994. Structural characteristics of old-growth hemlock-hardwood forest in relation to age. Ecology 75, 370-386. https://doi.org/10.2307/1939541.

Van der Maaten E., 2012. Climate sensitivity of radial growth in European beech (*Fagus sylvatica* L.) at different aspects in southwestern Germany. Trees 26, 777–788. https://doi.org/10.1007/s00468-011-0645-8.

Vasile, D., Petritan, A.M., Tudose, N.C., Toiu, F.L., Scarlatescu, V., Petritan, I.C., 2017. Structure and spatial distribution of dead wood in two temperate old-growth mixed European beech forests. Not. Bot. Horti. Agrobo. 45(2), 639-645. https://doi.org/10.15835/nbha45210829.

Vera, F.W.M., 2000. Grazing ecology and forest history. CABI Publishing, Oxon.

Vilanova, E., Ramírez-Angulo, H., Torres-Lezama, A., Aymard, G., Gámez, L., Durán, C., Hernández, L., Herrera, R., van der Heijden, G., Phillips, O.L., Ettl, G.E., 2018. Environmental drivers of forest structure and stem turnover across Venezuelan tropical forests. PLoS ONE 13(6), e0198489. https://doi.org/10.1371/journal.pone.0198489.

Vitousek, P.M., Porder, S., Houlton, B.Z., Chadwick, O.A., 2010. Terrestrial phosphorus limitation: mechanisms, implications, and nitrogen–phosphorus interactions. Ecol. Appl. 20, 5-15. https://doi.org/10.1890/08-0127.1.

von Oheimb G., Westphal C., Tempel H., Härdtle W., 2005. Structural pattern of a near-natural beech forest (*Fagus sylvatica*) (Serrahn, north-east Germany). Forest Ecology and Management 212: 253-263. https://doi.org/10.1016/j.foreco.2005.03.033.

Weber, J., 2000. Geostatistische Analyse der Struktur von Waldbeständen am Beispiel ausgewählter Bannwälder in Baden-Württemberg. Berichte Freiburger Forstliche Forschung Heft 20. FVA Baden-Württemberg. Freiburg. 133 pp.

Wijdeven, S.M.J., 2004. Stand dynamics in Fontainebleau. Dynamics in beech forest structure and composition over 17 years in La Tillaie forest reserve, Fontainebleau, France. Green World Research, Alterra, Wageningen University.

Wolf, A., 2005. Fifty year record of change in tree spatial patterns within a mixed deciduous forest. For. Ecol. Manage. 215, 212-223. https://doi.org/10.1016/j.foreco.2005.05.021.

Zenner, E.K., Hibbs, D.E., 2000. A new method for modelling the heterogeneity of forest structure. For. Ecol. Manage. 129 (1), 75-87. https://doi.org/10.1016/S0378-1127(99)00140-1.

Zhiwei, X., Xinghua, W., 2010. Research for information extraction based on wrapper model algorithm. 2010 Second International Conference on Computer Research and Development. Kuala Lumpur, Malaysia, pp. 652-655.

8. Tables

Table 1. Basic statistics of the environmental variables in the 112 experimental plots

Type/ Source	**Code**	**Description**	**Mean**	**Min.**	**Max.**	**Std. Dev**
Terrain/ PNOA Lidar	SLP	Slope based on a digital elevation model (%)	22.95	4.03	42.04	7.85
	ASP	Aspect based on a digital elevation model (º)	172.18	2.85	355.08	110.42
	CU	Curvature	-0.15	-5.24	7.06	1.32
	PLC	Plan curvature	-0.11	-3.96	4.22	0.87
	PRC	Profile curvature	0.03	-2.84	1.94	0.62
	TSI	Terrain shape index	0.00	-0.24	0.18	0.05
	WI	Wetness index	9.57	7.24	16.43	1.92
	SR_SS	Potential incoming solar radiation in summer solstice (kJ m^2 $year^{-1}$)	5994.34	4996.97	6806.93	344.71
	SR_EQ	Potential incoming solar radiation in equinox (kJ m^2 $year^{-1}$)	3153.88	2081.49	4440.32	517.70
	SR_WS	Potential incoming solar radiation in winter solstice (kJ m^2 $year^{-1}$)	633.48	314.96	1530.76	288.35
	DHN	Euclidean distance to hydrographic network	1415.66	0.00	3676.96	887.35
Climate/ World Clim	BIO01	Annual mean temperature (ºC)	8.67	5.90	10.90	1.11
	BIO02	Mean diurnal range (Mean of monthly (max temp - min temp)) (ºC)	10.03	9.20	10.60	0.30
	BIO03	Isothermality (BIO02/ BIO07) (*100) (ºC)	40.33	39.00	42.00	0.67
	BIO04	Temperature seasonality (std. Dev. *100) (ºC)	499.23	456.70	524.10	15.21
	BIO05	Max temperature of warmest month (ºC)	22.86	20.80	24.80	0.87
	BIO06	Min temperature of coldest month (ºC)	-1.70	-4.50	0.90	1.14
	BIO07	Temperature annual range (BIO05- BIO06) (ºC)	24.57	22.60	25.70	0.70
	BIO08	Mean temperature of wettest quarter (ºC)	6.01	2.70	8.70	1.23
	BIO09	Mean temperature of driest quarter (ºC)	15.25	12.90	17.10	0.93
	BIO10	Mean temperature of warmest quarter (ºC)	15.31	12.90	17.20	0.95
	BIO11	Mean temperature of coldest quarter (ºC)	2.65	-0.30	5.30	1.19
	BIO12	Annual precipitation (mm)	900.09	775.00	1062.00	63.27
	BIO13	Precipitation of wettest month (mm)	113.72	102.00	132.00	6.75
	BIO14	Precipitation of driest month (mm)	44.90	37.00	52.00	3.46
	BIO15	Precipitation seasonality (Coef. of variation) (%)	25.95	23.00	32.00	1.97
	BIO16	Precipitation of wettest quarter (mm)	305.04	270.00	360.00	20.42
	BIO17	Precipitation of driest quarter (mm)	159.82	136.00	184.00	11.36
	BIO18	Precipitation of warmest quarter (mm)	163.37	136.00	185.00	10.57
	BIO19	Precipitation of coldest quarter (mm)	250.75	206.00	320.00	27.15
Soil/ LUCAS topsoil chemical and physical properties	Ph_$CaCl_2$	Soil pH in $CaCl_2$ 0.01 M solution (cmol+ kg^{-1})	5.46	0.00	6.09	0.62
	Ph_H_2O	Soil pH in H_2O solution ((cmol+ kg^{-1})	5.96	0.00	6.56	0.68
	Ph_H_2O_$CaCl_2$	Soil pH in water and pH in $CaCl_2$ 0.01M solution	0.51	0.00	1.03	0.16
	CEC	Cation-exchange capacity (cmol+ kg^{-1})	15.54	0.00	26.43	4.75
	$CaCO_3$	Calcium carbonate ($CaCO_3$) (g kg^{-1})	34.91	0.00	163.32	34.68
	C/N	C:N ratio (%)	14.39	10.38	16.26	0.82
	N	Nitrogen (N) (g $kg^{-1)}$	3.16	0.00	6.48	1.21
	P	Phosphorus (P) (mg kg^{-1})	17.22	3.21	36.94	6.13
	K	Potassium (K) (mg kg^{-1})	142.92	0.00	210.87	38.85
	ACW	Available water capacity (%)	0.12	0.09	0.14	0.01
	BD	Bulk density (Mg m^{-3})	1.03	0.94	1.12	0.03
	CLAY	Clay content (%)	22.62	13.60	30.08	3.26
	COFG	Coarse fragments (%)	25.31	13.82	35.77	4.84
	SAND	Sand content (%)	41.62	24.29	64.71	7.23
	SILT	Silt content (%)	36.16	21.69	51.55	5.62
	USDA[1]	USDA soil textural classes	-	-	-	-
Soil/ SoilGrid	SC	Soil organic carbon content (Mg/ha)	86.04	58.00	129.00	14.59
	DB	Absolute deep to bed rock (cm)	1405.70	933.00	1881.00	203.23
	DB200	Depth of bedrock (R horizon) to 200 cm (cm)	194.62	169.00	200.00	6.75
	R	Probability occurrence of R horizon (%)	30.21	14.00	41.00	5.36
Soil/ SGM	Geo_unit[1]	Geological units	-	-	-	-
	Geo_lit_unit[1]	Lithological units	-	-	-	-
Soil/ SSM	LIT_dco[1]	Lithostratigraphy	-	-	-	-
	LIT_per[1]	Lithostratigraphy permeability	-	-	-	-
Soil/ESDB	WRB-Full[1]	Full soil code of the Soil typological units from the World Reference Base (WRB) for Soil Resources	-	-	-	-
	WRB-LEV[1]	Soil reference group of the Soil typological units from the World Reference Base (WRB) for Soil Resources	-	-	-	-

[1] qualitative variable.

Table 2. Individual-tree and stand-related structure indices used in the study

Class	Index (reference)	Formula	Explanation	Interpretation
Spatial tree distrib.	Aggregation index[1] (Clark and Evans, 1954)	$R=\frac{\bar{r}_{observed}}{E(r)}$; where $E(r)=1/2\sqrt{N/A}$; $R \in [0, 2.149]$	$\bar{r}_{observed}$ is the mean of the distances from the trees to their nearest neighbours, N is the number of trees of the stand, A is the area of the forest stand	$R > 1$ indicates regularity; $R < 1$ indicates clustering; $R = 1$ indicates random tree positions
	Contagion index[2] (Hui and Gadow, 2002)	$W_i=\frac{1}{n}\cdot\sum_{j=1}^{n} w_{ij}$; where $w_{ij}=\begin{cases}1\ if\ \alpha_{ij}<\alpha_0\\0\ if\ \alpha_{ij}\geq\alpha_0\end{cases}$; $W_i \in [0, 1]$	α_{ij} is the angle between trees i and j and a reference direction, α_0 = 72º	W_i = 0.00 indicates very regular distribution; W_i = 0.25 indicates regular; W_i = 0.50 indicates random; W_i = 0.75 indicates cluster; W_i = 1.00 indicates very irregular or clumped
	Mean Directional Index[2] (Corral-Rivas *et al*., 2006)	$MDI_i=\sqrt{\left(\sum_{j=1}^{n}\cos\alpha_{ij}\right)^2+\left(\sum_{j=1}^{n}\sin\alpha_{ij}\right)^2}$	α_{ij} is the angle between trees i and j and a reference direction	MDI_i > 1.799 denotes clustering; MDI_i = 1.799 in case of random tree positions; MDI_i = 0 in a complete square pattern
Plant richness and species diversity	Tree species richness[1]	TSR= $n_{observed}$	$n_{observed}$ is the number of tree species identified into the plot	
	Shrubs-herbaceous species richness[1]	S-HSR= $n_{observed}$	$n_{observed}$ is the number of shrubs or herbaceous species identified into the plot	
	Segregation index[1] (Pielou, 1977)	$S=1-\frac{N\cdot(b+c)}{v\cdot n+w\cdot m}$; $S \in [-1, 1]$	N is the number of trees of the stand, b is the number of trees of i species nearest to trees of j species, c is the number of trees of j species nearest to trees of i species, n is the is the number of trees of i species, m is the number of trees of j species, v = (m - b) + c, w = b + (n - c).	S < 0 indicates thorough mingling or association between species; S > 0 indicates segregation, i.e. spatial separation of species; S = 0 indicates randomness of species distribution
	Shannon index[1] (Shannon and Weaver, 1949)	$H'=-\sum_{i=1}^{n} p_i\cdot\log_2(p_i)$; $H' \in [0, \ldots]$	p_i is the probability of a randomly selected tree belonging to species i, n is the number of tree species in the stand	H' = 0 if there is only one species; H' = $\log_2(Z)$ if there are Z species with equal relative proportions.
	Simpson index[1] (Simpson, 1949)	$1-D=1-\sum_{i=1}^{n} p_i^2$; $D \in [0, 1]$	p_i is the probability of a randomly selected tree belonging to species i, n is the number of tree species in the stand	D = 0 if there is only one species in the community; D = 1 if there are infinite species in the community.
	Mingling index[2] (Gadow, 1993)	$M_i=\frac{1}{n}\cdot\sum_{j=1}^{n} v_{ij}$; where $v_{ij}=\begin{cases}1\ if\ sp_i\neq sp_j\\0\ if\ sp_i=sp_j\end{cases}$; $M_i \in [0, 1]$	sp_i is the species of the reference tree i, sp_j is the species of the jth neighbour tree	M_i = 0.00 implies no mingling; M_i = 0.25 indicates weak mingling; M_i = 0.50 implies moderate mingling; M_i = 0.75 indicates high mingling; M_i = 1.00 indicates total mingling
Tree dimensions and vertical structure	Diameter differentiation[2] (Füldner, 1995)	$TD_i=1-\frac{\min(dbh_i, dbh_j)}{\max(dbh_i, dbh_j)}$; $TD_i \in [0, 1]$	dbh_i is the diameter of tree i, dbh_j is the diameter of tree j	TD_i = 0-0.3, small differentiation; TD_i = 0.3-0.5, moderate; TD_i = 0.5-0.7, large; TD_i = 0.7-1, very large differentiation
	Mean diameter differentiation[2] (Pommerening, 2002)	$TDM_i=1-\frac{1}{n}\sum_{j=1}^{n}\left(\frac{\min(dbh_i, dbh_j)}{\max(dbh_i, dbh_j)}\right)$; $TDM_i \in [0, 1]$	dbh_i is the diameter of reference tree i, dbh_j is the diameter of its nearest neighbour j, n is the effective number of trees in the plot	TDM_i = 0-0.3, small differentiation; TDM_i = 0.3-0.5, moderate; TDM_i = 0.5-0.7, large; TDM_i = 0.7-1, very large differentiation
	Height differentiation[2] (Pommerening, 2002)	$TH_i=1-\frac{\min(h_i, h_j)}{\max(h_i, h_j)}$; $TH_i \in [0, 1]$	h_i is the height of tree i, h_j is the height of the nearest neighbour tree j	TH_i = 0-0.3, small differentiation; TH_i = 0.3-0.5, moderate; TH_i = 0.5-0.7, large; TH_i = 0.7-1, very large differentiation
	Mean height differentiation[2] (Gadow, 1999)	$TH_i=1-\frac{\min(h_i, h_j)}{\max(h_i, h_j)}$; $TH_i \in [0, 1]$	h_i is the height of reference tree i, h_j is the height of its nearest neighbour j, n is the effective number of trees in the plot.	THM_i = 0-0.3, small differentiation; THM_i = 0.3-0.5, moderate; THM_i = 0.5-0.7, large; THM_i = 0.7-1, very large differentiation

[1] Stand-related-indices. [2] Individual-tree-related indices

Table 2 (Cont.). Individual-tree and stand-related structure indices used in the study

Class	Index (reference)	Formula	Explanation	Interpretation
Tree dimensions and vertical structure	Diametrical dominance index[2] (Hui *et al*., 1998)	$Ud_i = \frac{1}{n} \cdot \sum_{j=1}^{n} v_j$; where $v_j = \begin{cases} 1 \ if \ d_i > d_j \\ 0 \ otherwise \end{cases}$; $Ud_i \in [0, 1]$	dbh_i is the diameter of the reference tree *i*, dbh_j is the diameter of the *j*th neighbour tree (*n*=4)	Ud_i = 0 implies strongly suppressed tree; Ud_i = 0.25 moderately suppressed; Ud_i = 0.50 co-dominant; Ud_i = 0.75 dominant; Ud_i = 1.00 very dominant
	Height dominance index[2] (Hui *et al*., 1998)	$Uh_i = \frac{1}{n} \cdot \sum_{j=1}^{n} v_j$; where $v_j = \begin{cases} 1 \ if \ h_i > h_j \\ 0 \ otherwise \end{cases}$; $Uh_i \in [0, 1]$	h_i is the height of the reference tree *i*, h_j is the height of the *j*th neighbour tree (*n*=4)	Uh_i = 0 implies strongly suppressed tree; Uh_i = 0.25 moderately suppressed; Uh_i = 0.50 co-dominant; Uh_i = 0.75 dominant; Uh_i = 1.00 very dominant
	Shannon vertical index[1] (Pretzsch, 1996)	$H'_V = -\sum_{i=1}^{s} \sum_{j=1}^{z} p_{ij} \log_2 \left(p_{ij}\right)$; $H_V' \in [0, \ldots]$	p_{ij} is the proportion of *i* species in the *j* stratum, *s* is number of species in the plot, *z* is the number of height strata	H'_V = 0 if there is only one species and one stratum; $H'_V = \log_2(Z)$ if there are Z species with equal relative proportions in the strata.
	Shannon stratified index[1] (Weber, 2000)	$H'_{str} = -\sum_{i=1}^{n} \left(\frac{h \cdot p_i}{n \cdot h_i}\right) \cdot \log_2 \left(\frac{h \cdot p_i}{n \cdot h_i}\right)$; $H_{str}' \in [0, \ldots]$	p_i is the proportion of trees of the *i* stratum, *n* is the number of strata, *h* is the height of the forest, h_i is the height of *i* stratum	H'_{str} = 0 if there is only one stratum; $H'_{str} = \log_2(Z)$ if there are Z strata with equal relative proportions
Stand density and average tree size	Number of trees per hectare[1]	$N = \frac{10000}{S_p} \sum_{i=1}^{i=n} n_i$	N is the number of trees per hectare (trees/ha), n_i is the number of trees per plot, S_p is the plot surface area in m^2	
	Basal area[1] (m^2/ha)	$G = \frac{2500 \cdot \pi}{S_p} \sum_{i=1}^{i=n} dbh_i^2$	*dbhi* is the diameter of tree i, S_p is the plot surface in m^2	
	Stocking level[1]	$StDeg_i = \frac{N_{\max}}{N}$	N is the number of trees per hectare (trees/ha), $N_{\max} = \exp\left(10.9 + 0.03 \cdot M\right) \cdot dg^{(-1.2716 - 0.0091 \cdot M)}$ (Condés *et al*., 2017), *M* is the Martonne aridity index *M*=*P*/ (*T*+10), being *P* annual precipitation in mm and *T* mean annual temperature in ºC	*StDeg*> 0.6 indicates overstocked; *StDeg*< 0.6 and > 0.35 indicate fully stocked; *StDeg* < 0.35 indicates understocked
	Hart-Becking index[1] (%)	$HB_i = \sqrt{20000 / N\sqrt{3}} \Big/ H_0$	HB_i is the Hart-Becking index (%), N is the number of trees per hectare and H0 is the dominant height	When *HBi* is greater, crowding is lower
	Dominant height[1] (m)	$H_0 = \sum_{i=1}^{i=n} h_0 \Big/ n_0$	h_0 is the height (m) of the n_0 thickest trees (the proportion of the 100 thickest trees per hectare of the plot)	
	Mean height[1] (m)	$Hm = \sum_{i=1}^{i=n} h_i \Big/ n_i$	h_i is the height (m) of the tree *i*, and n_i is the number of trees per plot	
Standing dead wood	Number of standing dead trees per hectare[1] (trees ha^{-1})	$N_{dead} = \frac{10000}{S_p} \sum_{i=1}^{i=n} n_{dead}$	n_{dead} is the number of dead trees per plot, S_p is the plot surface area in m^2.	
	Basal area of standing dead trees[1] (m^2 ha^{-1})	$G_{dead} = \frac{2500 \cdot \pi}{S_p} \sum_{i=1}^{i=n} dbhi_{dead}^2$	$Dbhi_{dead}$ is the diameter of dead tree *i*, S_p is the plot surface in m^2.	

[1] Stand-related-indices. [2] Individual-tree-related indices

Table 3. Values (mean, maximum, minimum and standard deviation) of the indices analyzed in this study.

Class	Abbr. and units	Index	Mean	Min.	Max.	Std. Dev
Spatial tree distrib.	R	Aggregation index	0.9277	0.3805	1.6482	0.2347
	W	Contagion index	0.5825	0.50	0.75	0.0461
	MDI	Mean directional index	2.2714	1.4023	2.8124	0.2072
Plant richness and species diversity	TSR	Tree species richness	1.4864	1	4	0.8187
	S-HSR	Shrub and herbaceous richness	5.9189	2	12	3.0938
	S	Segregation index	0.8323	0.1857	0.9277	0.0922
	H'	Shannon index	0.1431	0	1.0129	0.2582
	D	Simpson index	0.0813	0	0.5612	0.1533
	M	Mingling index	0.0722	0	0.7500	0.1433
Tree dimensions and vertical structure	TD	Diameter differentiation	0.2465	0.0450	0.6071	0.1052
	TDM	Mean diameter differentiation	0.2822	0.0625	0.5952	0.1140
	TH	Height differentiation	0.1393	0	0.3750	0.0880
	THM	Mean height differentiation	0.1869	0.0100	0.5000	0.1072
	Ud	Diametrical dominance index	0.5145	0.3500	0.5937	0.0266
	Uh	Height dominance index	0.5050	0.2965	0.5925	0.0870
	$H`_v$	Shannon vertical index	1.0394	0.0859	1.7462	0.2420
	$H`_{str}$	Shannon stratified index	1.1257	0.4417	1.2312	0.2158
Stand density and average tree size	N (trees ha^{-1})	Trees per hectare	1218.32	94	4200	775.09
	G (m^2 ha^{-1})	Basal area	44.57	15.35	178.70	17.27
	StDeg (%)	Stocking level	0.96	0.39	1.73	0.23
	HBi (%)	Hart-Becking index	21.11	10.84	46.66	6.17
	H_0 (m)	Dominant height	17.73	7.15	35.90	4.80
	Hm (m)	Mean height	14.18	6.80	33.21	4.14
Standing dead wood	N_{dead} (trees ha^{-1})	Trees dead per hectare	13.01	0	125	27.72
	G_{dead} (m^2 ha^{-1})	Basal area standing dead trees	0.1611	0	2.2138	0.3874
Canopy geometry and light regime	S_open (%)	Site openess	14.9759	11.8433	18.0711	1.7812
	LAI 4	Leaf Area Index 4	5.1864	4.6866	7.7566	1.1960
	LAI 5	Leaf Area Index 5	4.9593	4.5566	7.3133	1.1403
	BDR (MJ m^{-2} d^{-1})	Below canopy direct radiation	1.7583	1.1433	3.5801	0.8132
	BDifR (MJ m^{-2} d^{-1})	Below canopy diffuse radiation	2.1993	1.7933	3.3866	0.4368
	BTR (MJ m^{-2} d^{-1})	Below canopy total radiation	3.8573	2.7233	6.1203	1.1488
	BTR (%)	Below canopy total radiation as a percentage of BDR	13.1703	8.2800	17.1267	2.3197

Table 4. Results of the analysis of correlation between diversity indices

	R	*W*	*MDI*	*TSR*	*S-HSR*	*S*	*H'*	*D*	*M*	*TD*	*TDM*	*TH*	*THM*	*Ud*	*Uh*	*H'v*	*H'str*
R																	
W	-																
MDI	-	**0.8196** ***															
TSR	-	-	-														
S-HSR	-	0.1849 *	0.1958 *	-													
S	**0.8972** ***	-	-	-	-												
H'	-	-	-	-	-	-											
D	-	-	-	**0.8343** ***	-	-	-										
M	-	-	-	**0.7821** ***	-	-	0.1996 *	**0.9600** ***									
TD	-	-	0.2610 **	0.3045 **	**0.3877** ***	-	-	0.3142 ***	0.3194 ***								
TDM	-	-	0.2462 **	0.2013 *	**0.3740** ***	-	-	-	0.1957 *	**0.8095** ***							
TH	-	-	0.2338 *	0.3310 ***	0.3152 ***	-	-	**0.4108** ***	**0.4452** ***	**0.7455** ***	**0.6816** ***						
THM	-	-	0.2496 **	0.2086 *	**0.3711** ***	-	-	0.2713 **	0.3085 **	**0.6798** ***	**0.8112** ***	**0.8725** ***					
Ud	-	-	-	-	-	-	0.2253 *	-	-	-	-	-	-				
Uh	-	-	-	-	-	-	-	-	-	-	-	-	-	**0.5561** ***			
H'v	-	-	0.2234 *	**0.7501** ***	-	-	-	**0.6866** ***	**0.6032** ***	**0.3701** ***	0.3629 ***	0.3554 ***	0.3417 ***	-	-		
H'str	-	-	-	-	-	-	-	-	-	0.2502 **	0.3389 ***	-	0.2941 **	-	0.2186 *	**0.6738** ***	

*** denotes p-value < 0.001; ** denotes 0.001< p-value < 0.01; * denotes 0.01< p-value < 0.05; - denotes non-significant results

Note. Bold characters indicate correlation is significant at alpha level after Bonferroni correction (Bonferroni, 1936). *R*=Aggregation index; *W*=Contagion index; *MDI*=Mean directional index; *TSR*=Tree species richness; *S-HSR*=Shrub and herbaceous richness; *S*=Segregation index; *H`*= Shannon index; *D*=Simpson index; *M*= Mingling index; *TD*= Diameter differentiation; *TDM*=Mean diameter differentiation; *TH*=Height differentiation; *THM*=Mean height differentiation; *Ud*= Diametrical dominance index; *Uh*= Height dominance index; *H`v*= Shannon vertical index; *H`str*= Shannon stratified index.

Table 4 (Cont.). Results of the analysis of correlation between diversity indices

	N	*G*	*StDeg*	*HBi*	H_0	*Hm*	*N dead*	*G dead*	*S_open*	*BDR*	*BDifR*	*BTR*	*BTR%*
N									-	-	-	-	-
G	-								-	-	-	-	-
StDeg	-	**0.9578** ***							-	-	-	-	-
HBi	**-0.3973** ***	-0.2398 *	**-0.4001** ***						-	0.2890 *	-	0.3124 *	-
H_0	**-0.5457** ***	**0.4316** ***	0.2895 **	-0.3207 ***					-	-	-	-	-
Hm	**-0.4827** ***	**0.3977** ***	0.2529 **	-	**0.8619** ***				-	-	-	-	-
N dead	-	-	-	-	-	-			0.3036 *	-	0.2708 *	-	-
G dead	-	0.3063 ***	**0.3942** ***	-	-	-	**0.7610** ***		-	-	-	-	-
R	**-0.3891** ***	0.2117 **	-	-	**0.4163** ***	**0.5535** ***	-	-	-	-	-	-	-
W	**0.3413** ***	-	-	-	-	-	-	-	-	-	-	-0.2871 *	-0.3097 *
MDI	0.3399 ***	-	-	-	-	-	-	-	-	-	-	-0.2740 *	-0.2964 *
TSR	-	-	0.2697 **	-	-	-	-	-	-	-	-	-	-
S	**-0.3589** ***	0.3308 ***	0.2034 *	-	**0.3879** ***	**0.4955** ***	-	-	-	-	-	-	-
H'	-	0.3409 ***	0.3226 ***	-	-	-	-	-	-	-	-	-	-
M	-	-	**0.9965** ***	-	-	-	-	-	-	-	-	-	-
TD	-	-	0.3039 **	-	-	-	-	-	-	-	-	-	-
TH	-	-	**0.4325** ***	-	-	-	-	-	-	-	-	-	-
THM	-	-	0.2981 **	-	-	-	-	-	-	-	-	-	-
H'v	-	0.2031 *	0.2146 *	-	-	-	-	-	-	-	-	-	-

*** denotes p-value < 0.001; ** denotes 0.001< p-value < 0.01; * denotes 0.01< p-value < 0.05; - denotes non-significant results

Note. Bold characters indicate correlation is significant at alpha level after Bonferroni correction (Bonferroni, 1936). *N*=Number of trees per hectare; *G*=Basal area ($m^2.ha^{-1}$); *StDeg*=Stocking level; *HBi*=Hart-Becking index (%); H_0=Dominant heigh (m); *Hm*=Mean height (m); N_{dead}=Number of standing dead trees per hectare ($trees.ha^{-1}$); G_{dead}=Basal area of standing dead trees ($m^2.ha^{-1}$); *R*=Aggregation index; *W*=Contagion index; *MDI*=Mean directional index; *TSR*=Tree species richness; *S*=Segregation index; *H`*= Shannon index; *M*= Mingling index; *TD*= Diameter differentiation; *TH*=Height differentiation; *THM*=Mean height differentiation; *H`v*= Shannon vertical index; *H`str*= Shannon stratified index; S*_open*= Site openness (%); *BDR*= Below canopy direct radiation (MJ m^{-2} d^{-1}); *BDifR*= Below canopy diffuse radiation (MJ m^{-2} d^{-1}); *BTR*= Below canopy total radiation (MJ m^{-2} d^{-1}); *BTR%*= Below canopy total radiation as percentage of BDR.

Table 5. Preliminary analysis of the RF models to predict structure indices as a function of environmental variables

Class	Abbr.	Index	RF Model	
			R^2	Nº variables
Spatial tree distribution	**R**	**Aggregation index**	**0.16**	**2**
	W	Contagion index	0.17	6
	MDI	Mean directional index	-	-
Plant richness and species diversity	**TSR**	**Tree species richness**	**0.25**	**1**
	S-HSR	**Shrub and herbaceous richness**	**0.38**	**6**
	S	Segregation index	0.04	1
	H'	**Shannon index**	**0.32**	**7**
	D	Simpson index	0.32	13
	M	Mingling index	0.32	13
Tree dimensions and vertical structure	***TD***	**Diameter differentiation**	**0.27**	**7**
	TDM	Mean diameter differentiation	0.17	11
	TH	**Height differentiation**	**0.26**	**7**
	THM	Mean height differentiation	0.22	7
	Ud	Diametrical dominance index	0.24	6
	Uh	Height dominance index	0.17	3
	H'_v	Shannon vertical index	0,15	2
	H'str	**Shannon stratified index**	**0.22**	**1**
Density and average tree size	*N* (trees ha^{-1})	Trees per hectare	0.44	8
	G (m^2 ha^{-1})	Basal area	0.08	1
	***StDeg* (%)**	**Uniform angle index**	**0.22**	**16**
	HBi (%)	Hart-Becking index	0.14	3
	H_0 (m)	**Dominant height**	**0.51**	**8**
Standing dead wood	N_{dead} (trees ha^{-1})	Trees dead per hectare	0.39	6
	G_{dead} (m^2 ha^{-1})	**Basal area standing dead trees**	**0.38**	**2**

R^2= coefficient of determination of de model; Nº variables= number of variables retained by the RF model. The RF selected models within each Diversity Class are shown in bold.

Table 6. Variables included in the RF models, including type and normalized relative importance

Class	RF Model	Type	Variable	Normalized Relative Importance (VIM_N, %)	Accumulated VIM_N (%)	R^2	RMSE
Spatial tree distribution	Aggregation index	Soil	Geo_lit_unit	99.00	99.00	0.16	0.22
		Soil	USDA	1.00	100.00		
Plant richness and species diversity	Tree species richness	Climate	BIO03	100.00	100.00	0.25	0.72
	Shrub-herbaceous species richness	Soil	$pH\_H2O\_CaCl_2$	34.66	34.66	0.38	1.75
		Climate	BIO11	21.61	56.27		
		Climate	BIO01	20.21	76.48		
		Climate	BIO15	15.23	91.71		
		Soil	WRB-LEV	7.95	99.66		
		Soil	WRB-Full	0.34	100.00		
	Shannon_sp	Soil	SAND	18.14	18.14	0.32	0.22
		Soil	K	17.53	35.67		
		Terrain	SR_WS	17.09	52.76		
		Soil	N	13.64	66.39		
		Terrain	WI	13.62	80.01		
		Climate	BIO03	10.91	90.92		
		Soil	DB	9.08	100.00		
Tree dimensions and vertical structure	Shannon vertical index	Climate	BIO03	100.00	100.00	0.22	0.22
	Füldner diameter differentiation	Climate	SR_WS	25.31	25.31	0.27	0.09
		Climate	BIO07	25.19	50.50		
		Soil	DB	25.17	75.66		
		Climate	BIO03	10.50	86.16		
		Soil	Geo_unit	8.91	95.07		
		Soil	WRB-Full	4.73	99.80		
		Soil	USDA	0.20	100.00		
	Füldner height differentiation	Soil	CEC	20.36	20.36	0.26	0.08
		Soil	$pH\_H2O\_CaCl_2$	19.41	39.77		
		Soil	SILT	19.32	59.09		
		Climate	BIO07	17.30	76.39		
		Climate	BIO19	17.25	93.64		
		Climate	BIO03	4.53	98.17		
		Soil	WRB-LEV	1.83	100.00		
Density and average tree size	Stocking level	Soil	BD	12.82	12.82	0.22	0.21
		Soil	P	10.34	23.16		
		Soil	C/N	10.00	33.16		
		Soil	CEC	8.26	41.42		
		Soil	N	7.99	49.41		
		Climate	BIO01	7.90	57.31		
		Terrain	PLC	7.75	65.06		
		Terrain	WI	6.50	71.56		
		Climate	BIO09	6.23	77.80		
		Climate	BIO19	6.10	83.90		
		Climate	SR_WS	5.50	89.39		
		Climate	BIO16	5.30	98.22		
		Climate	BIO15	3.52	92.92		
		Soil	Geo_unit	1.37	99.60		
		Soil	WRB-LEV	0.33	99.93		
		Soil	USDA	0.07	100.00		
	Dominant height	Climate	BIO04	24.03	24.03	0.51	3.84
		Climate	BIO05	21.77	45.80		
		Climate	BIO02	18.99	64.79		
		Terrain	SLP	17.16	81.94		
		Climate	BIO15	8.23	90.17		
		Soil	WRB-Full	5.39	95.56		
		Soil	WRB-LEV	4.44	100.00		
Standing dead wood	Basal area of standing dead trees	Climate	BIO02	99.00	99.00	0.38	0.20
		Climate	BIO15	1.00	100.00		

Geo_lit_unit=Lithological units; USDA=Soil textural class; BIO03=Isothermality (ºC); $Ph\_H_2O\_CaCl_2$=Soil pH in water and pH in $CaCl_2$; BIO11=Mean temperature of coldest quarter (ºC); BIO01=Annual mean temperature (ºC); BIO15=Precipitation seasonality (%); WRB-LEV=Soil reference group from World Reference Base (WRB);WRB-FULL=Full soil code from the World Reference Base (WRB); SAND=Sand content (%); K=Potassium (K) (mg kg-1); SR_WS=Potential incoming solar radiation in winter solstice (KJ m^2 $year^{-1}$); N= Nitrogen (N) (g kg^{-1}); WI= Wetness index; DB=Absolute depth to bed rock (cm); Geo_unit=Geological units; CEC=Cation-exchange capacity (cmol+ kg^{-1}); SILT=Silt content (%); BIO07=Temperature annual range (ºC); BIO19=Precipitation of coldest quarter (mm); BD= Bulk density (Mg m^{-3});P=Phosphorus (P) (mg kg^{-1});C/N C:N ratio (%); PLC=Plan curvature; BIO09=Mean temperature of driest quarter (ºC); BIO16=Precipitation of wettest quarter (mm); BIO04= temperature seasonality (ºC); BIO05=Max temperature of warmest month (ºC); BIO02=Mean diurnal range (ºC); SLP=slope.

Supplementary Table

Table S1. Current values of the climatic variables analyzed and predictions for the different climate change scenarios (RCP 4.5 and RCP 8.5) and different time horizons (2050 and 2070).

Variable	Current				2050 RCP 4.5				2050 RCP 8.5				2070 RCP 4.5				2070 RCP 8.5			
	Mean	**Min**	**Max**	**SD**	**Mean**	**Min**	**Max**	**SD**	**Mean**	**Min**	**Max**	**SD**	**Mean**	**Min**	**Max**	**SD**	**Mean**	**Min**	**Max**	**SD**
BIO01	8.3	2.2	13.8	1.8	9.7	3.6	15.0	1.8	10.4	4.2	15.6	1.7	10.0	3.8	15.3	1.8	11.2	5.0	16.3	1.7
BIO02	9.9	7.3	11.0	0.5	10.3	7.6	11.5	0.5	9.9	7.2	11.1	0.6	10.4	7.6	11.6	0.5	10.1	7.3	11.3	0.6
BIO03	40.2	38.0	44.0	0.9	40.3	38.0	44.0	0.9	37.9	35.0	42.0	1.0	40.4	38.0	44.0	0.9	37.8	35.0	42.0	1.0
BIO04	497.5	384.9	547.2	27.4	515.7	397.0	572.6	29.6	545.2	418.9	608.3	31.6	519.5	401.3	579.4	30.2	559.1	427.4	624.4	33.2
BIO05	22.4	16.8	25.3	1.2	24.3	18.5	27.3	1.2	25.2	19.3	28.4	1.3	24.7	18.8	27.8	1.3	26.4	20.4	29.6	1.3
BIO06	-2.0	-7.5	5.1	2.0	-1.0	-6.5	6.0	1.9	-0.6	-6.0	6.4	1.9	-0.8	-6.3	6.2	1.9	0.1	-5.4	7.0	1.9
BIO07	24.4	18.5	26.9	1.3	25.4	19.1	28.3	1.4	25.2	19.3	28.8	1.4	25.5	19.1	28.6	1.5	26.3	19.7	29.4	1.5
BIO08	5.6	-2.8	12.1	2.2	6.2	-1.6	13.3	2.7	7.1	-1.3	13.6	2.3	6.8	-1.4	13.6	2.5	7.3	-0.6	14.4	2.8
BIO09	14.9	9.3	18.8	1.5	16.6	10.9	20.2	1.4	17.4	11.9	21.0	1.4	16.8	11.2	20.3	1.3	18.4	12.8	21.9	1.3
BIO10	15	9.3	19.1	1.5	16.6	10.9	20.5	1.5	17.7	11.9	21.4	1.4	17.0	11.2	20.8	1.4	18.7	12.8	22.3	1.4
BIO11	2.3	-3.6	9.1	2.0	3.6	-2.4	10.2	2.0	3.8	-2.1	10.4	2.0	3.8	-2.2	10.4	2.0	4.4	-1.5	11.0	2.0
BIO12	931.1	718.0	1358.0	95.9	860.2	666.0	1264.0	89.5	839.5	648.0	1222.0	88.1	851.9	654.0	1248.0	88.7	821.8	635.0	1208.0	85.9
BIO13	116.5	90.0	158.0	10.1	108.6	83.0	150.0	9.8	112.9	87.0	158.0	10.3	111.5	85.0	153.0	10.0	113.6	87.0	152.0	9.5
BIO14	46.2	32.0	73.0	5.0	42.0	30.0	65.0	4.4	34.1	24.0	53.0	3.7	39.9	28.0	63.0	4.3	33.6	24.0	52.0	3.7
BIO15	25.8	21.0	34.0	2.2	26.8	22.0	38.0	2.7	31.4	27.0	42.0	2.4	27.1	22.0	39.0	2.7	32.0	27.0	42.0	2.4
BIO16	313.5	244.0	447.0	30.5	294.9	229.0	433.0	31.6	303.5	238.0	439.0	30.5	294.7	230.0	427.0	29.9	294.6	229.0	426.0	30.5
BIO17	164.1	123.0	244.0	15.7	145.3	111.0	212.0	12.3	132.5	99.0	195.0	12.9	147.2	109.0	218.0	14.0	128.7	96.0	188.0	12.5
BIO18	167.7	126.0	244.0	14.4	145.4	112.0	212.0	12.3	136.8	109.0	195.0	10.9	149.9	117.0	218.0	12.5	132.2	105.0	188.0	10.6
BIO19	261.4	189.0	415.0	38.6	251.3	181.0	401.0	37.7	252.5	183.0	402.0	37.5	248.1	179.0	394.0	36.8	255.2	185.0	405.0	37.9

BIO01= Annual mean temperature (ºC); BIO02= Mean diurnal range (ºC); BIO03= Isothermality (ºC); BIO04= Temperature seasonality (ºC); BIO05= Max temperature of warmest month (ºC); BIO06= Min temperature of coldest month (ºC); BIO07= Temperature annual range (ºC); BIO08= Mean temperature of wettest quarter (ºC); BIO09= Mean temperature of driest quarter (ºC); BIO10=Mean temperature of warmest quarter (ºC); BIO11= Mean temperature of coldest quarter (ºC); BIO12= Annual precipitation (mm); BIO13= Precipitation of wettest month (mm); BIO15= Precipitation seasonality (%); BIO16= Precipitation of wettest quarter (mm); BIO17= Precipitation of driest quarter (mm); BIO18= Precipitation of warmest quarter (mm); BIO19= Precipitation of coldest quarter (mm).

56

9. Figure Captions

Figure 1. Location of the study area.

Figure 2. Aggregation index results. Data are shown for each plot and ordered by increasing value.

Figure 3. Height-diameter dominance and differentiation modes for all plots.

Figure 4. Illustration of the spatially and temporally explicit maps of structural features derived from the RF models. Example for the standing deadwood basal area.

Supplementary Figures

Figure S1. Marginal response curves for variables included in the ten RF models that accumulate 75% of the relative importance for current environmental conditions. Variables are ordered by their contribution to the model (importance score)

Figure S2. Spatially-explicit-maps of structural features derived from the RF models and projections for the year 2050 under two climate change scenarios (moderate scenario-RCP 4.5 and pessimistic scenario-RCP 8.5).

Fig 1.

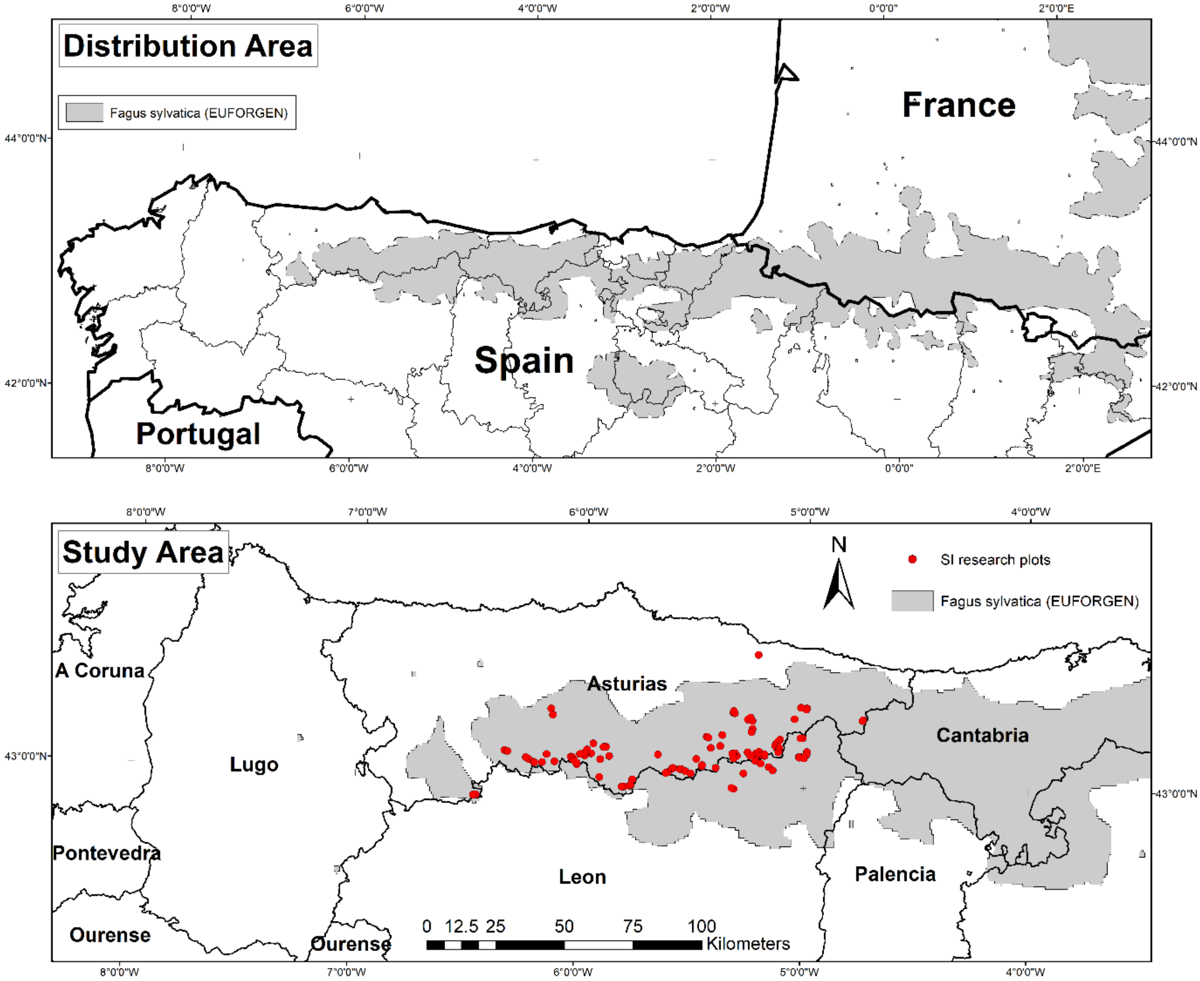
Distribution Area
Fagus sylvatica (EUFORGEN)
France
Spain
Portugal
Study Area
SI research plots
Fagus sylvatica (EUFORGEN)
N
A Coruna
Lugo
Pontevedra
Ourense
Ourense
Asturias
Cantabria
Leon
Palencia
0 12.5 25 50 75 100
Kilometers

Fig 2.

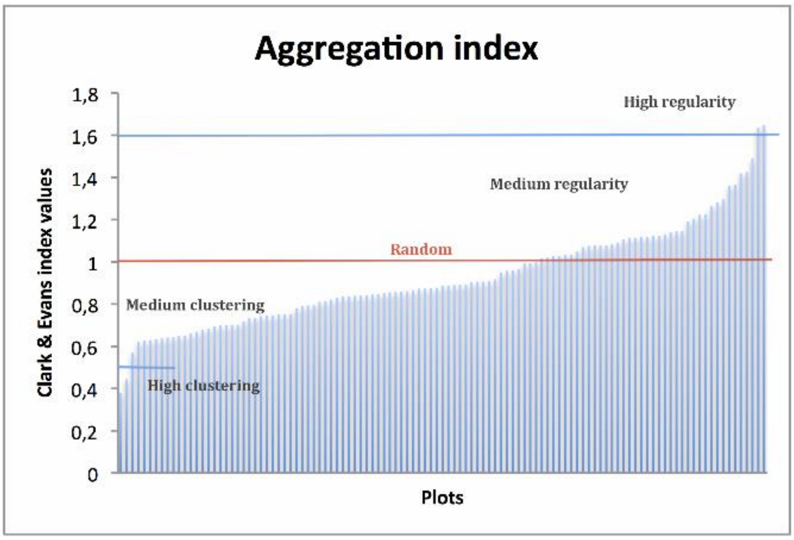
Aggregation index
Clark & Evans index values
Plots
1,8
1,6
1,4
1,2
1
0,8
0,6
0,4
0,2
0
High regularity
Medium regularity
Random
Medium clustering
High clustering

Fig 3.

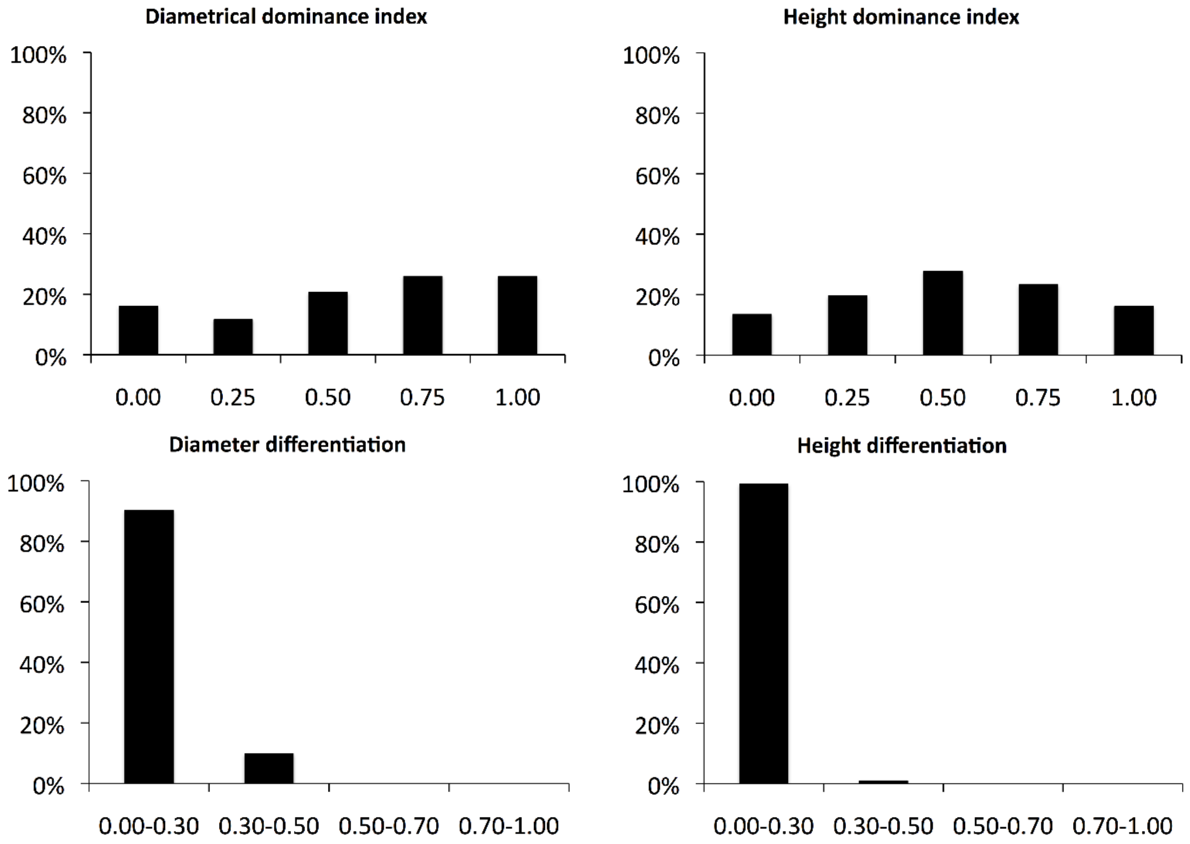
Diametrical dominance index
100%
80%
60%
40%
20%
0%
0.00
0.25
0.50
0.75
1.00
Height dominance index
Diameter differentiation
0.00-0.30
0.30-0.50
0.50-0.70
0.70-1.00
Height differentiation

Fig 4.

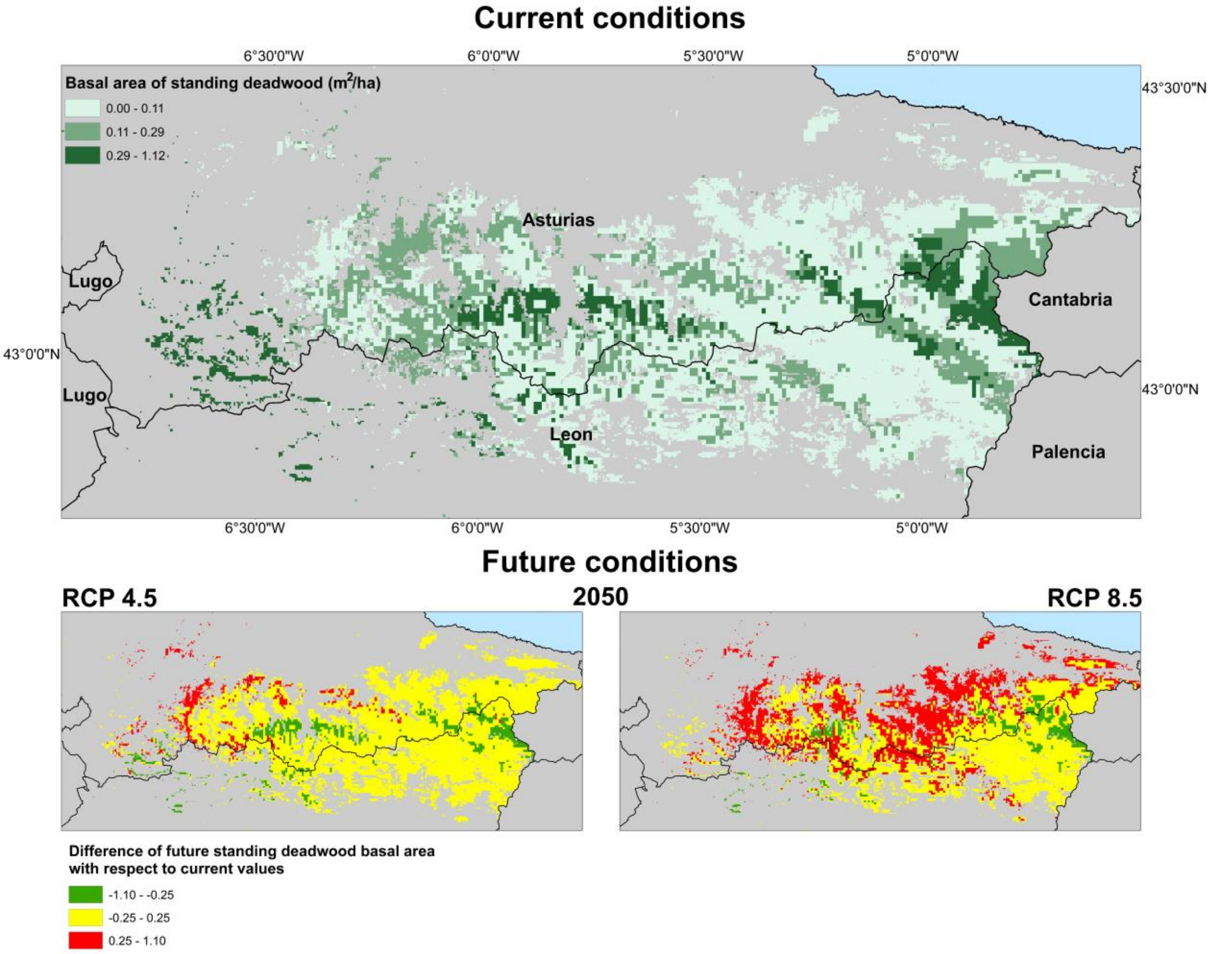
Current conditions
Basal area of standing deadwood (m2/ha)
0.00 - 0.11
0.11 - 0.29
0.29 - 1.12
6°30'0"W
6°0'0"W
5°30'0"W
5°0'0"W
43°30'0"N
43°0'0"N
Asturias
Lugo
Cantabria
Leon
Palencia
Future conditions
RCP 4.5
2050
RCP 8.5
Difference of future standing deadwood basal area with respect to current values
-1.10 - -0.25
-0.25 - 0.25
0.25 - 1.10

Figure S1.

Diversity class: Spatial tree distribution

RF model: Aggregation index

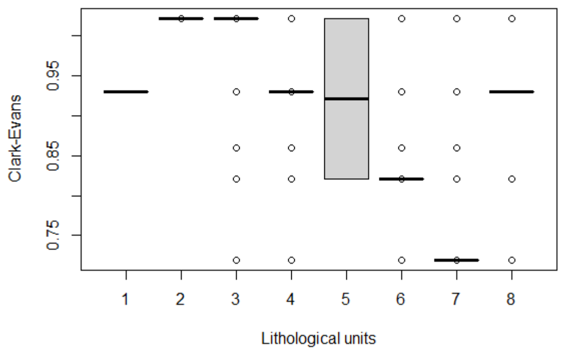

Description of lithological units

1.- Other granites
2.- Slates, greywackes, quartzites and conglomerates
3.- Quartzites, slates, sandstones and limestones
4.- Conglomerates, sandstones, slates and limestones. Coal
5.- Conglomerates, sandstones, limestones, plasters and versicolor clays
6.- Dolomites, limestones and marls. Sandstones
7.- Sandstones, slates and limestones
8.- Others

Diversity class: Plant richness and species diversity

RF model: Tree richness

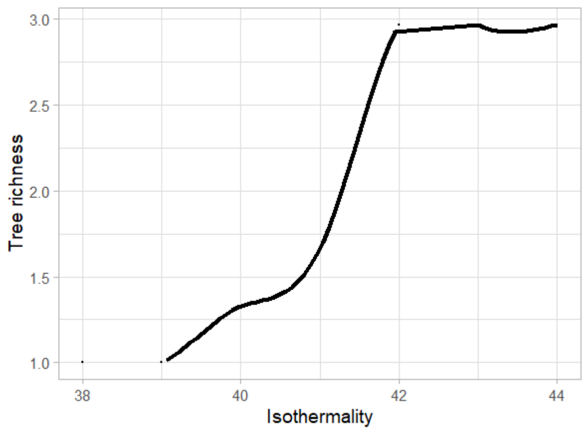

Diversity class: Plant richness and species diversity

RF model: Shrub-herbaceous species richness

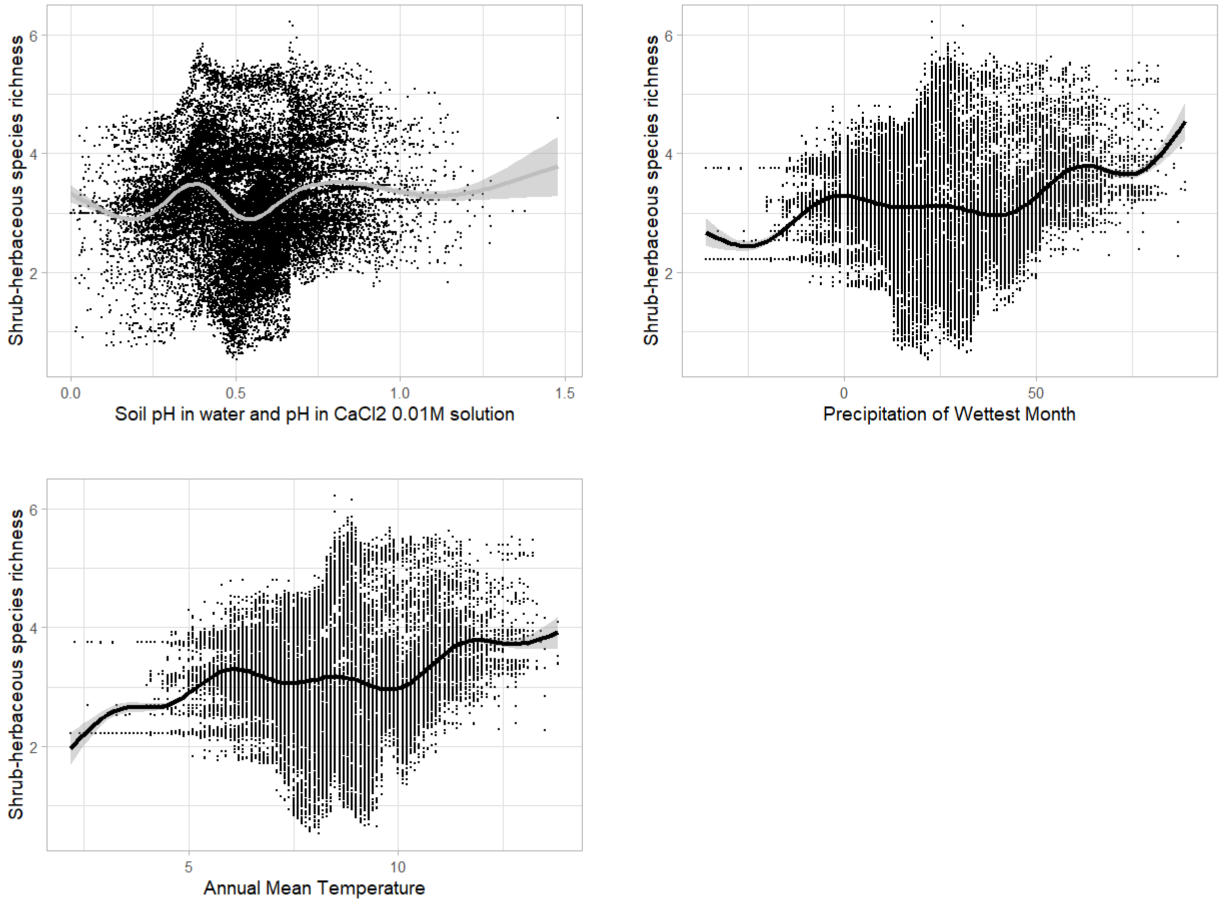

Diversity class: Plant richness and species diversity

RF model: Shannon index

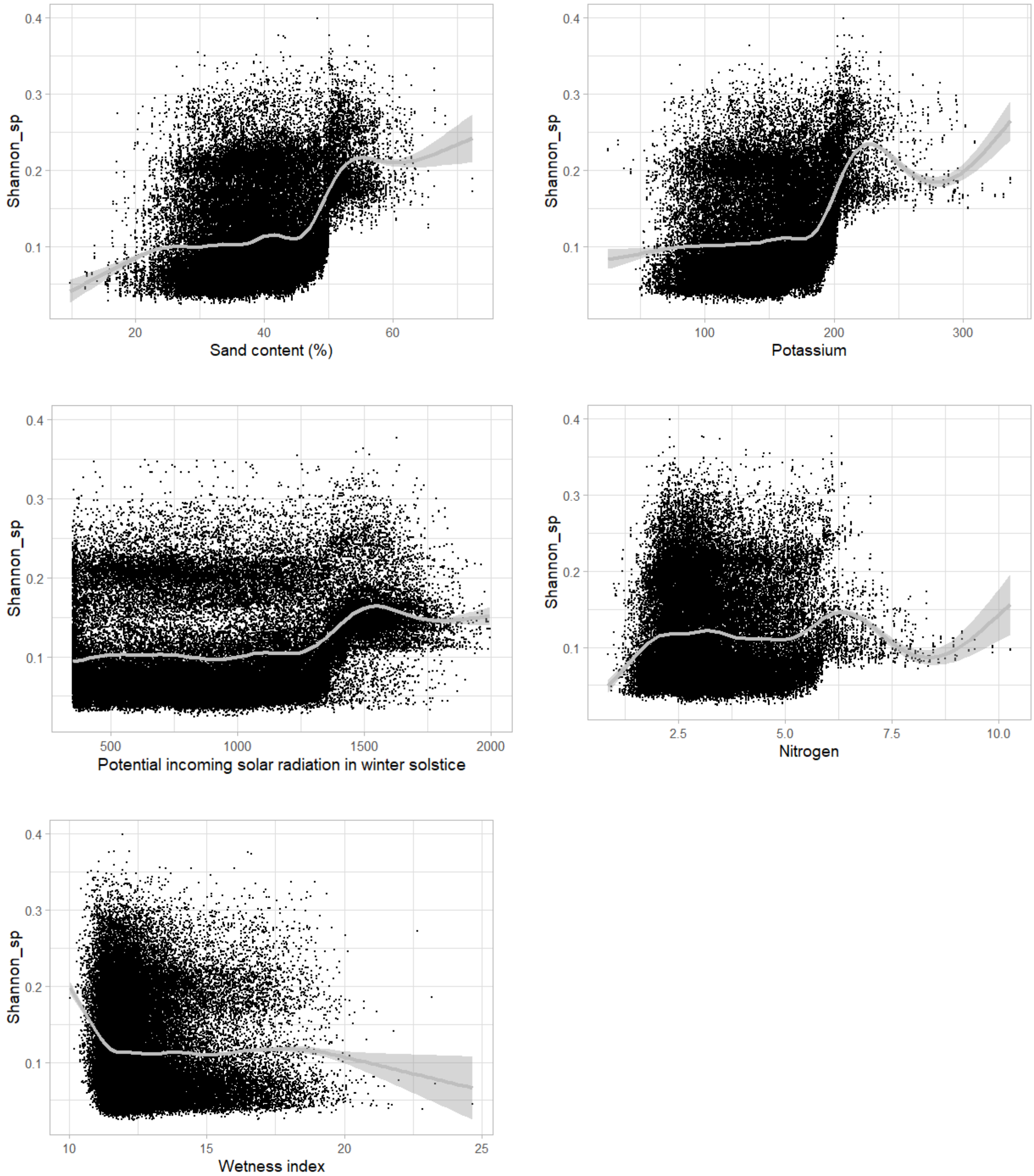

Diversity class: Tree dimensions and vertical structure

RF model: Shannon vertical index

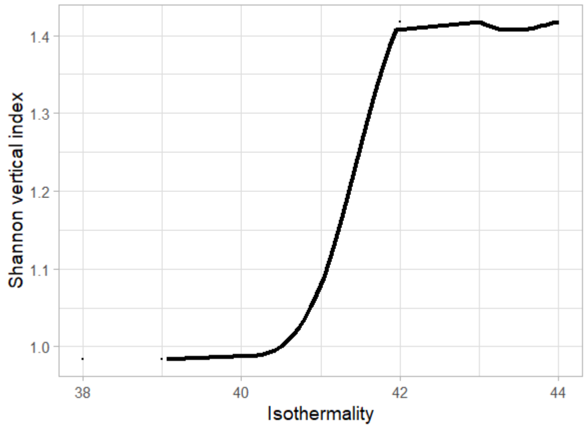

Diversity class: Tree dimensions and vertical structure

RF model: Diameter differentiation index

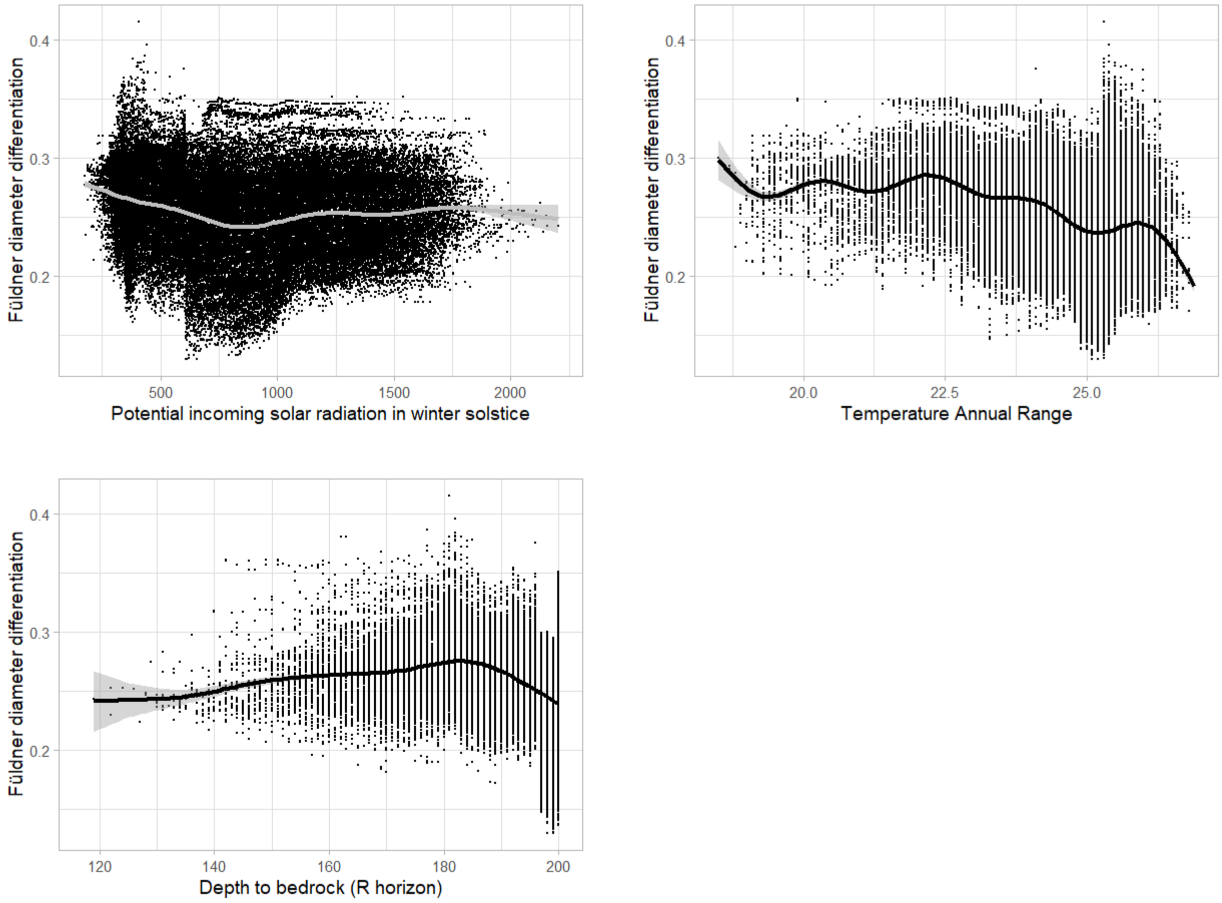

Diversity class: Tree dimensions and vertical structure

RF model: Height differentiation index

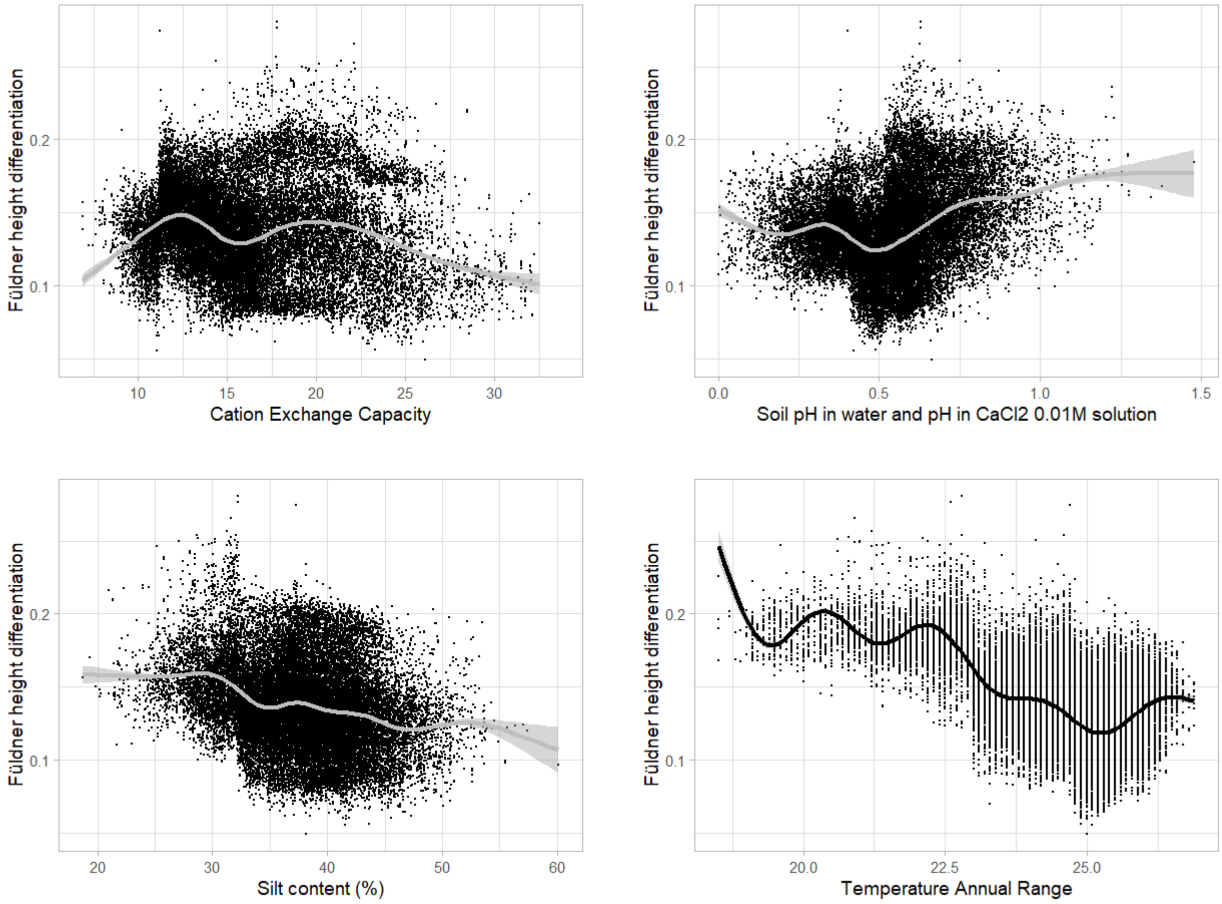

Diversity class: Standing dead wood

<u>RF model</u>: Basal area standing dead trees

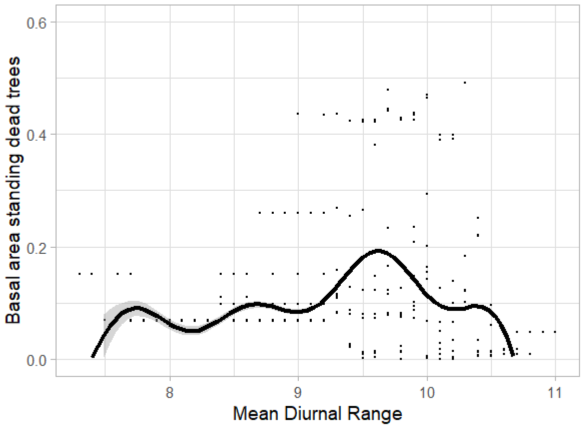

1204

Diversity class: Density and average tree size

<u>**RF model**</u>: Stocking level

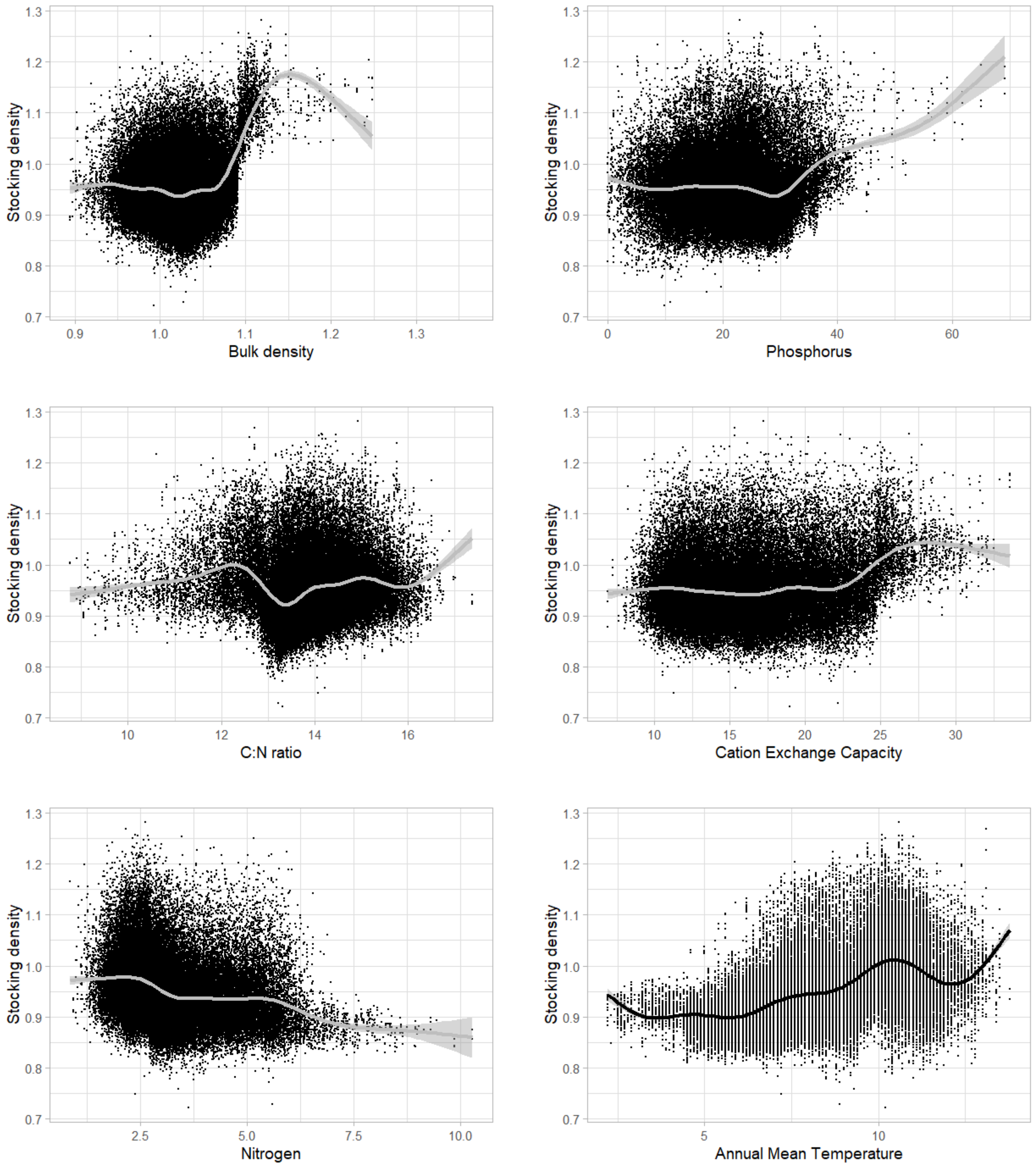

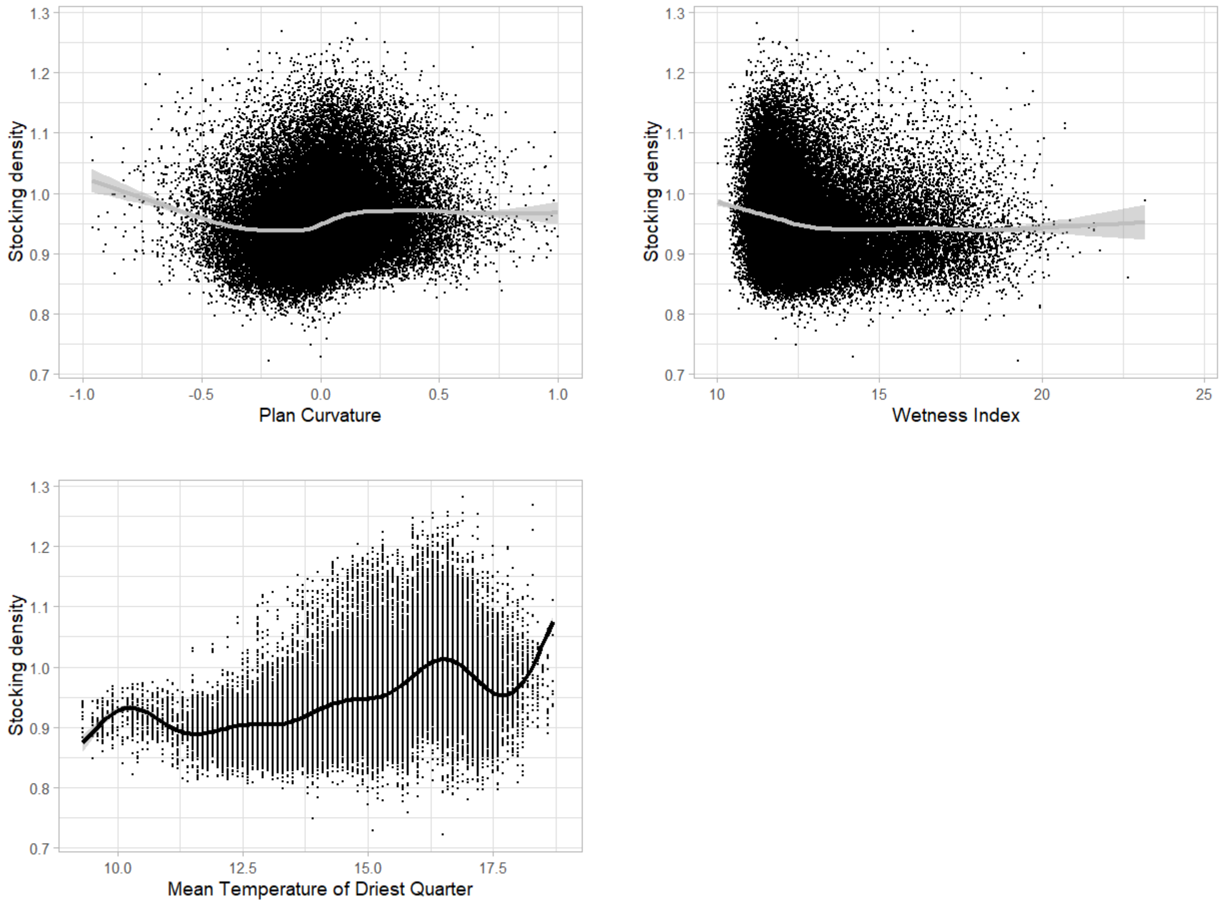

Stocking density
Plan Curvature
Stocking density
Wetness Index
Stocking density
Mean Temperature of Driest Quarter

1205

Diversity class: Density and average tree size

<u>RF model</u>: Dominant height

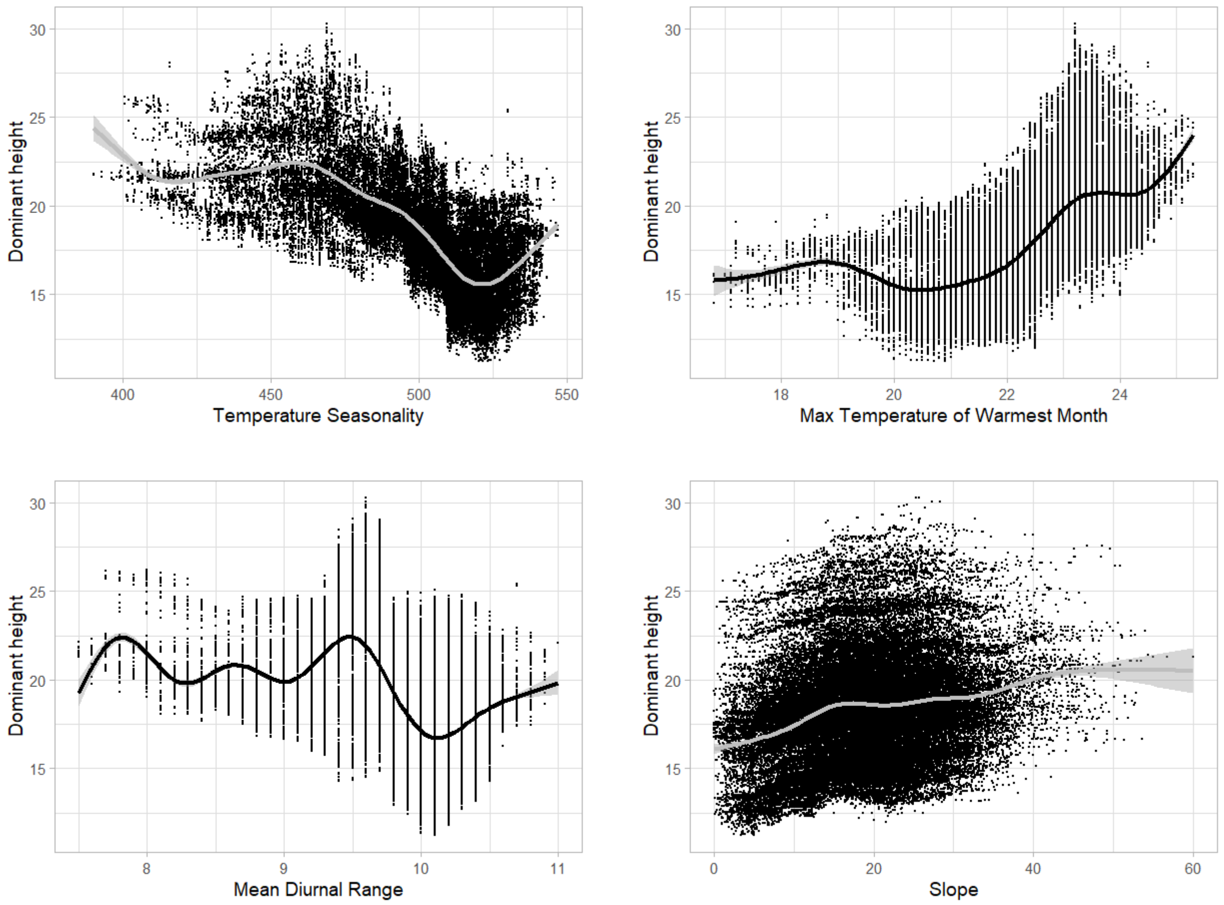

Figure S2.

Diversity class: Spatial tree distribution

<u>RF model</u>: Aggregation index or Clark-Evans index

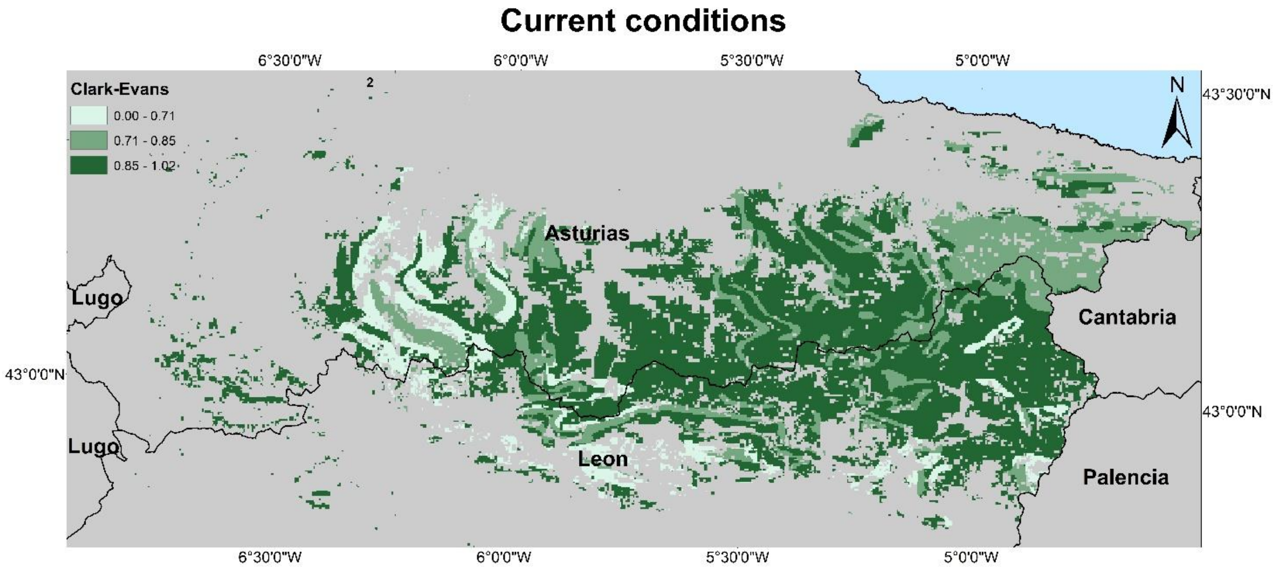

Note: RF model of this index does not incorporate climatic variables as predictor so future projections will be invariable

Diversity class: Plant richness and species diversity

RF model: Tree species richness

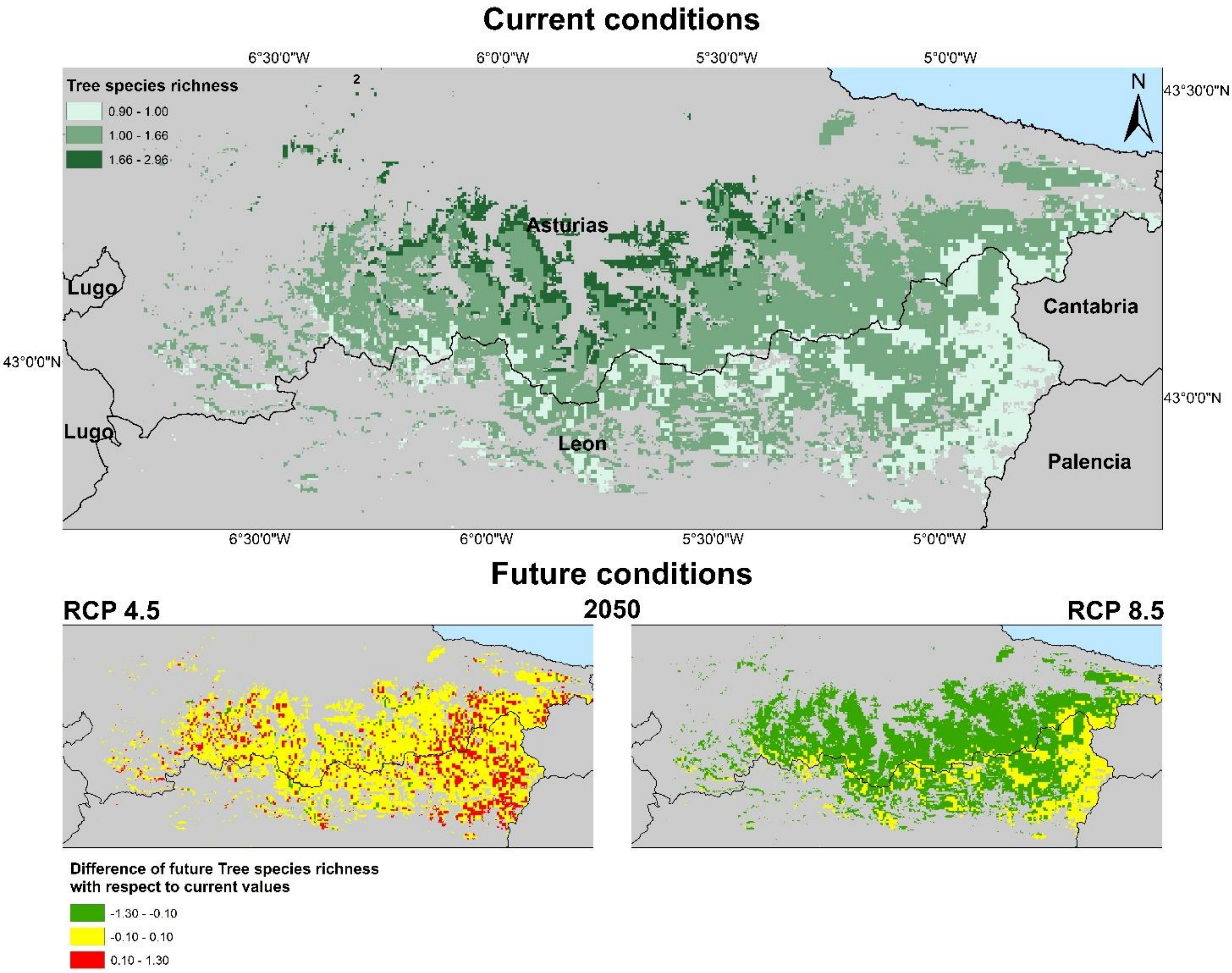

Diversity class: Plant richness and species diversity

RF model: Shrub-herbaceous species richness

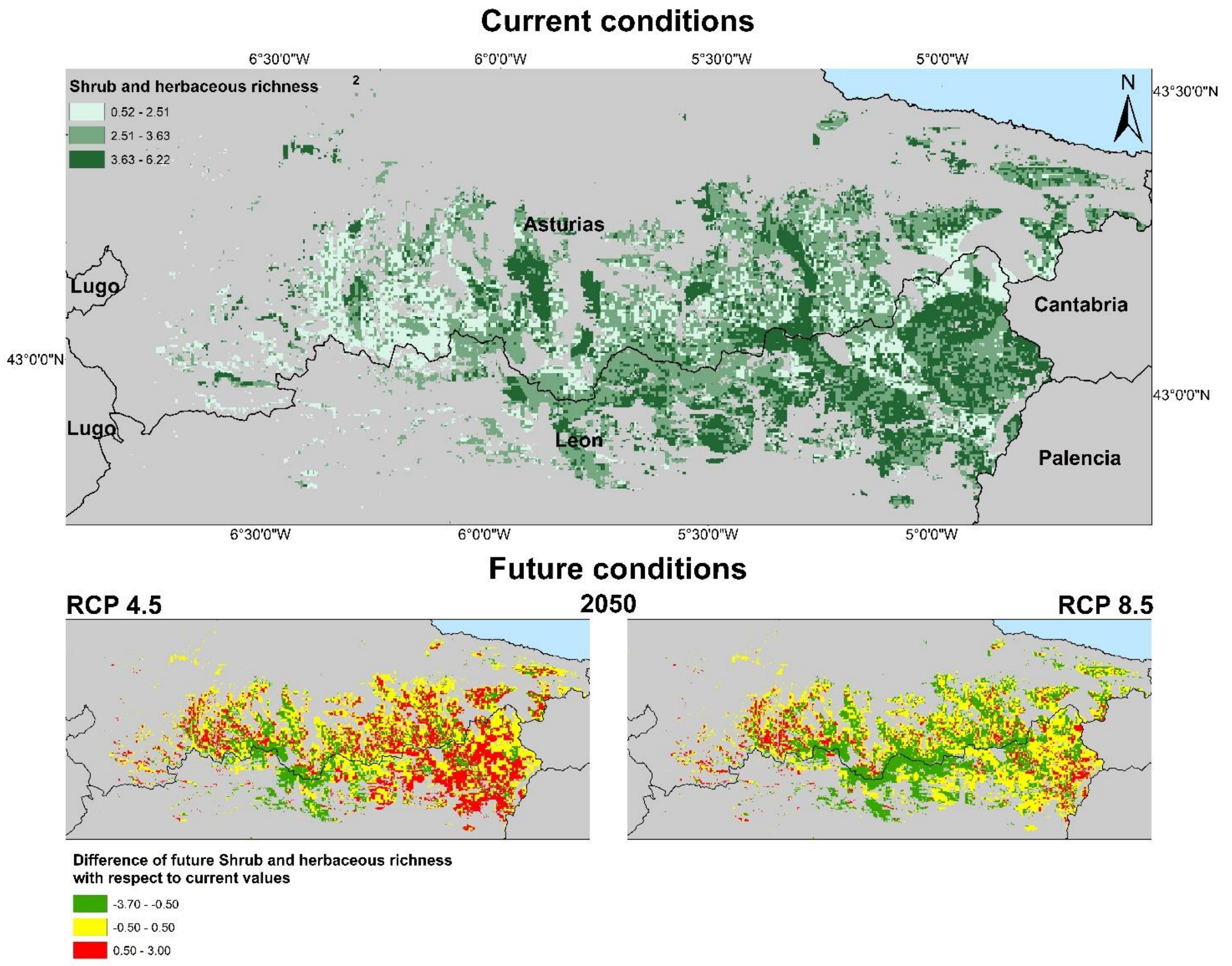

Diversity class: Plant richness and species diversity

RF model: Shannon_sp

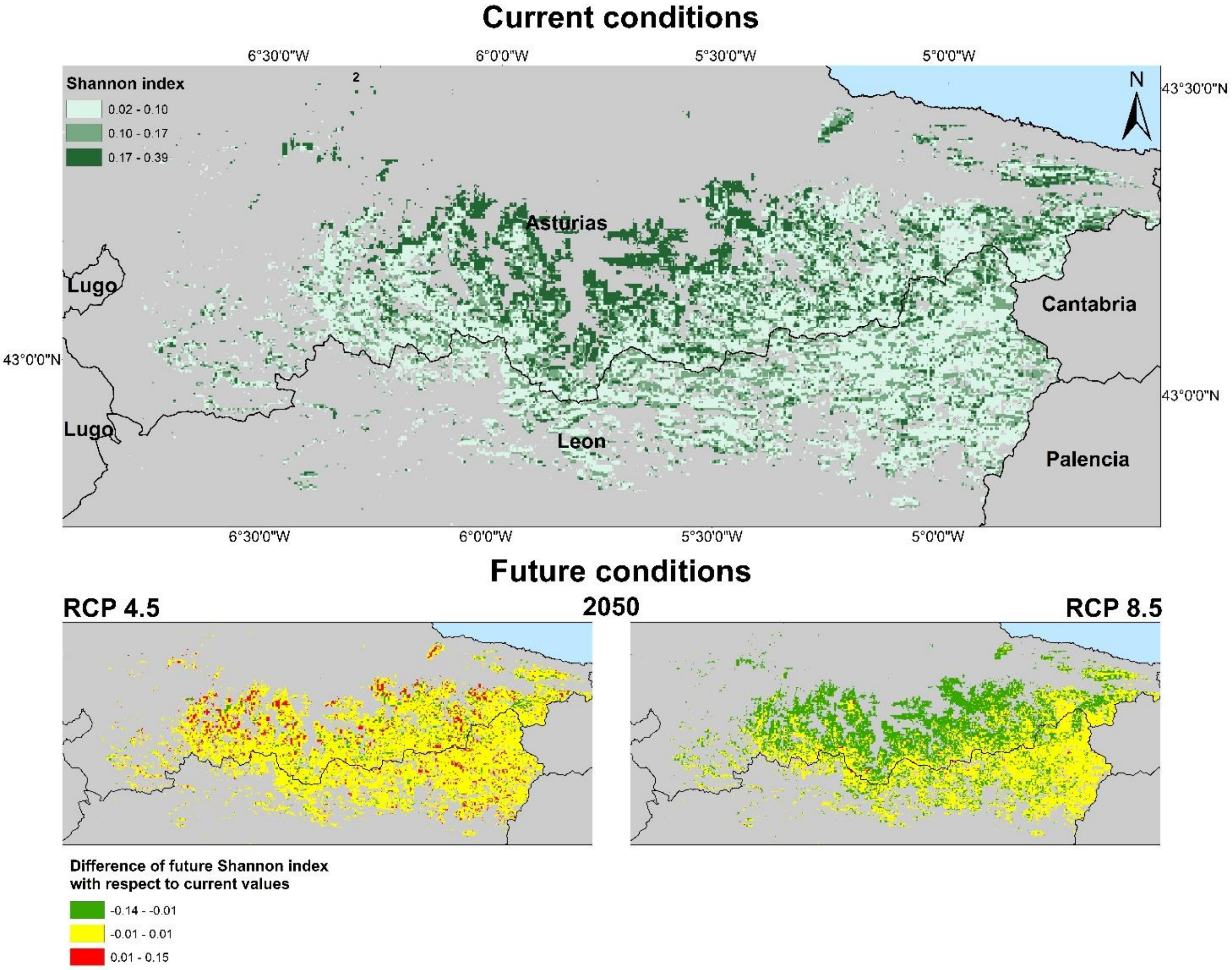

Diversity class: Tree dimensions and vertical structure

RF model: Shannon vertical index

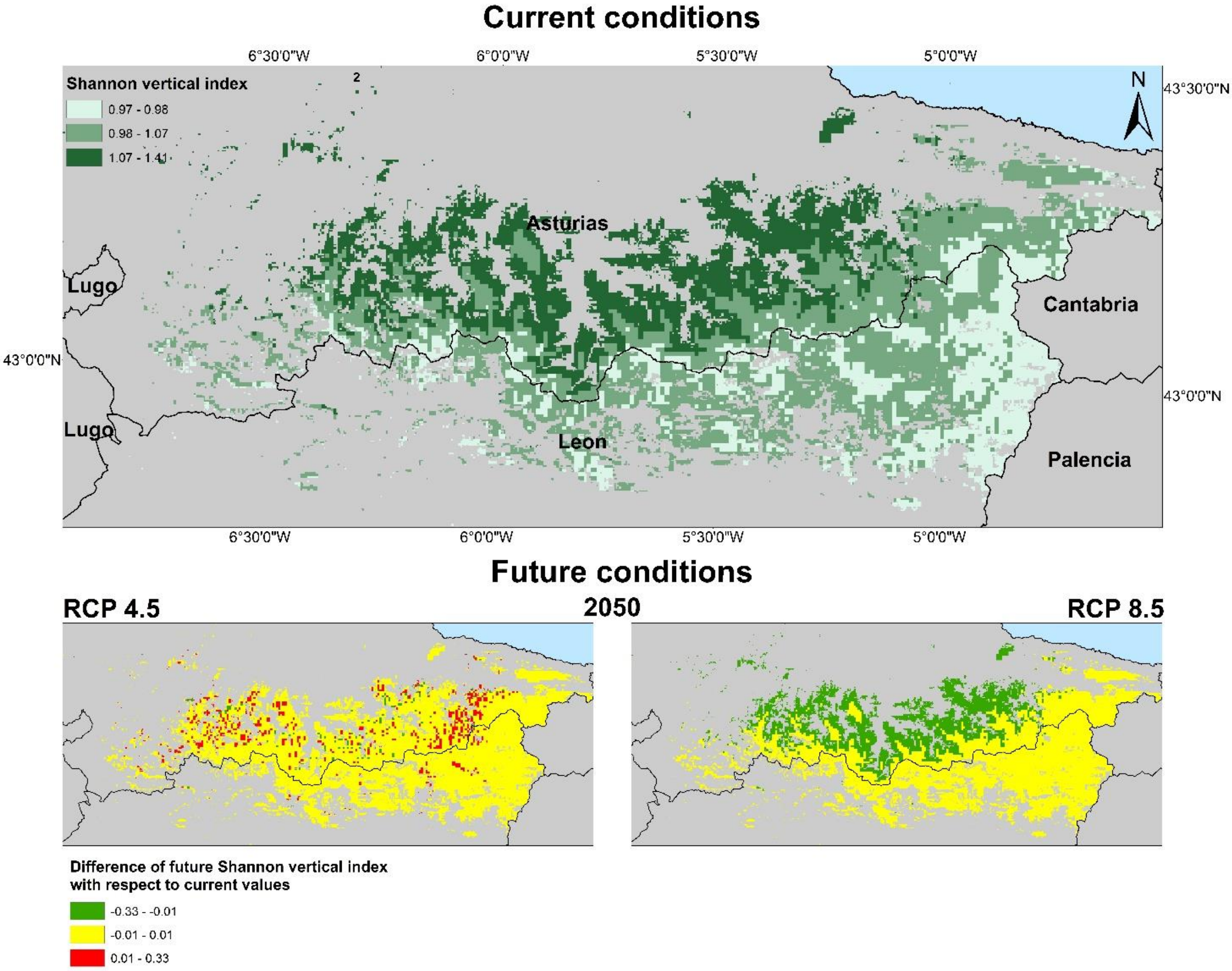

Diversity class: Tree dimensions and vertical structure

RF model: Füldner diameter differentiation

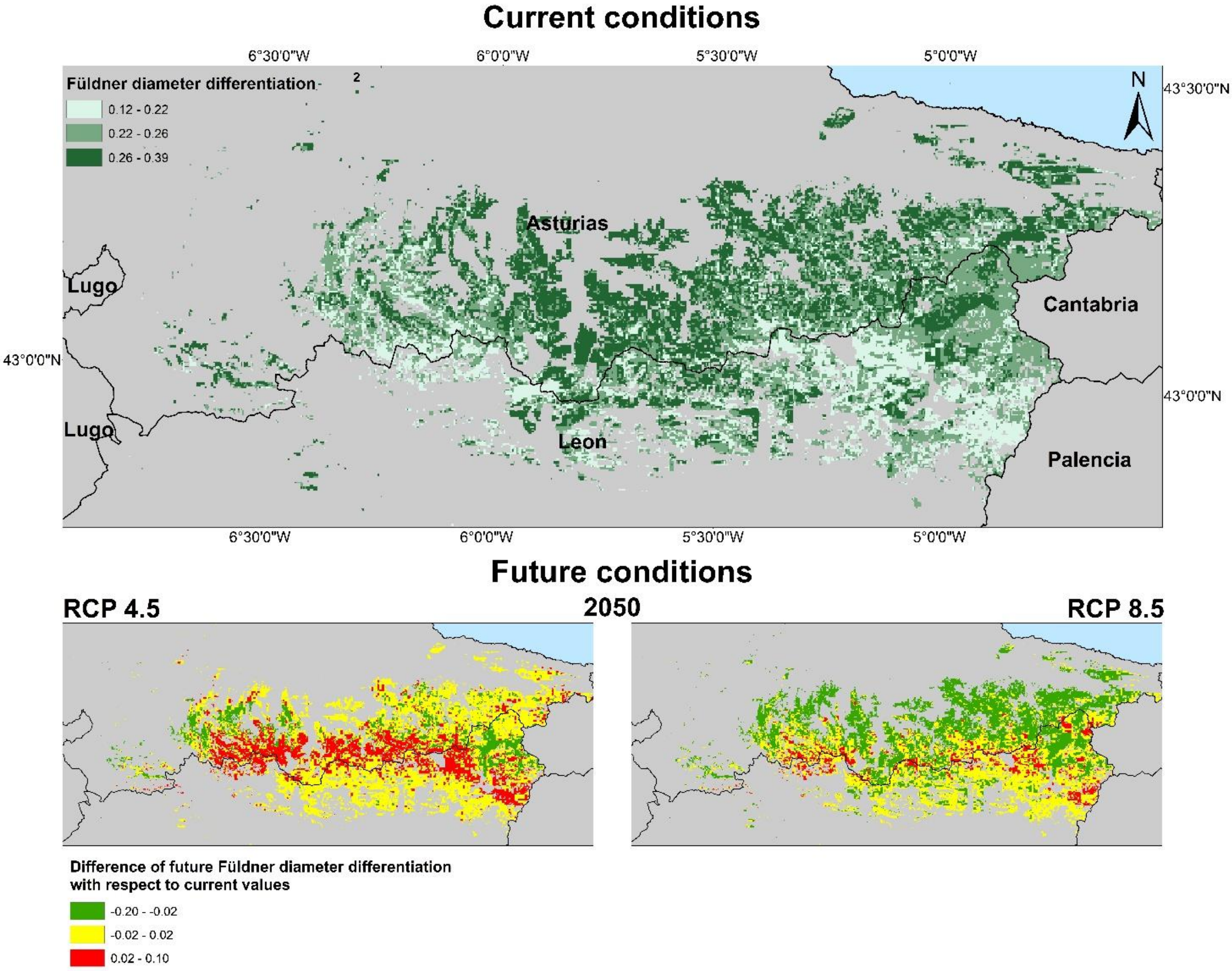

Diversity class: Tree dimensions and vertical structure

RF model: Füldner height differentiation

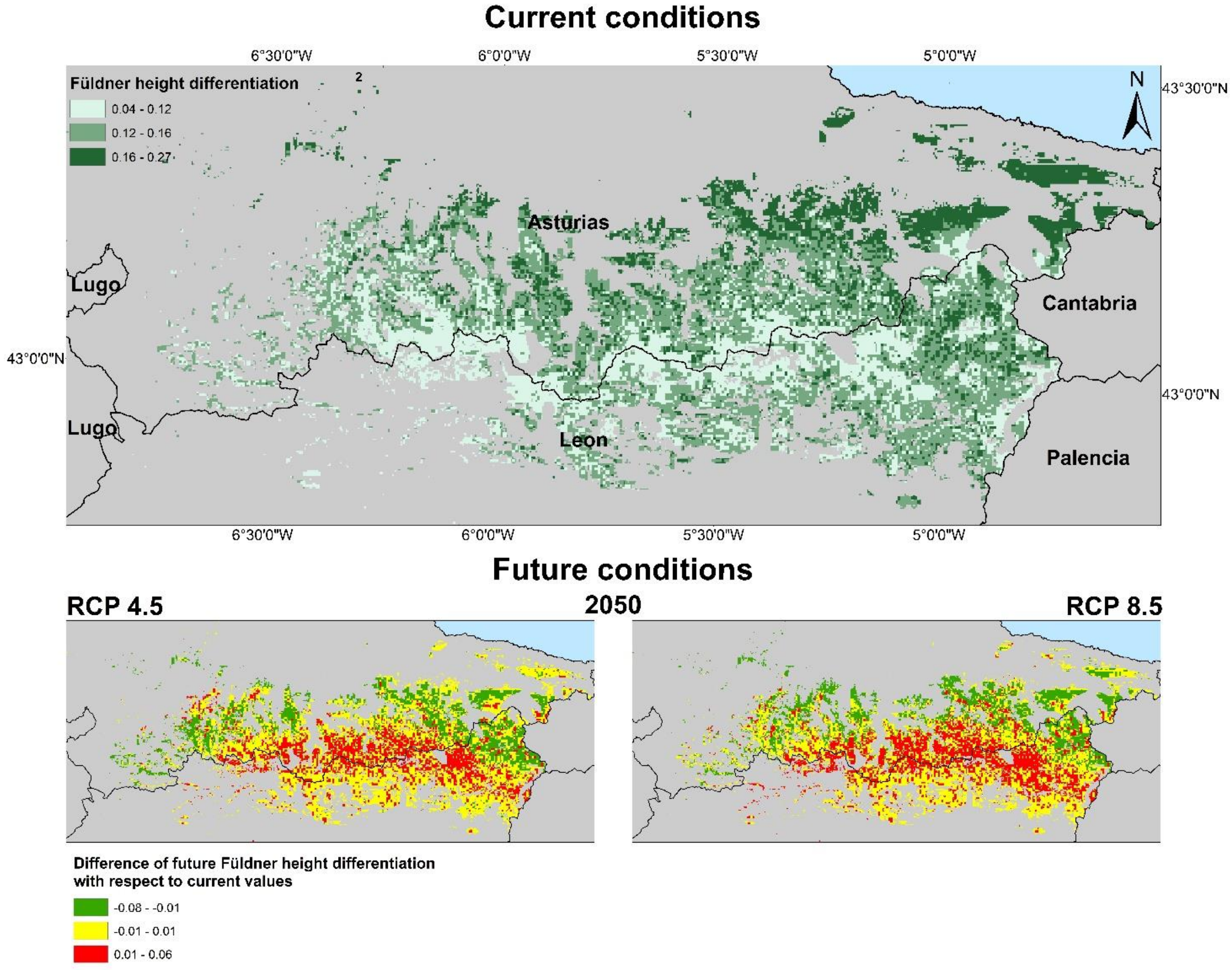

Diversity class: Standing dead wood

RF model: Basal area of standing dead trees

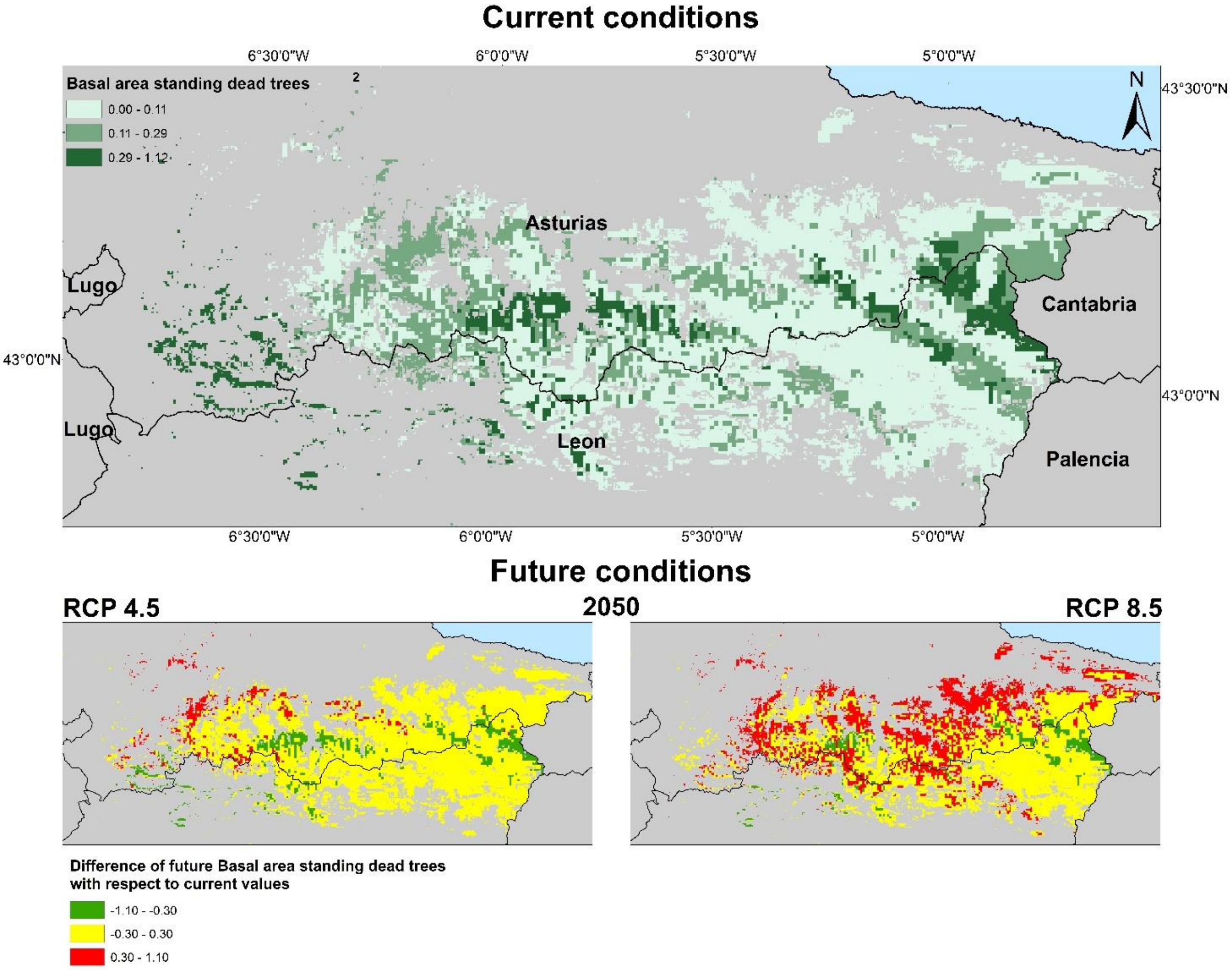

Diversity class: Density and average tree size

RF model: Stocking level

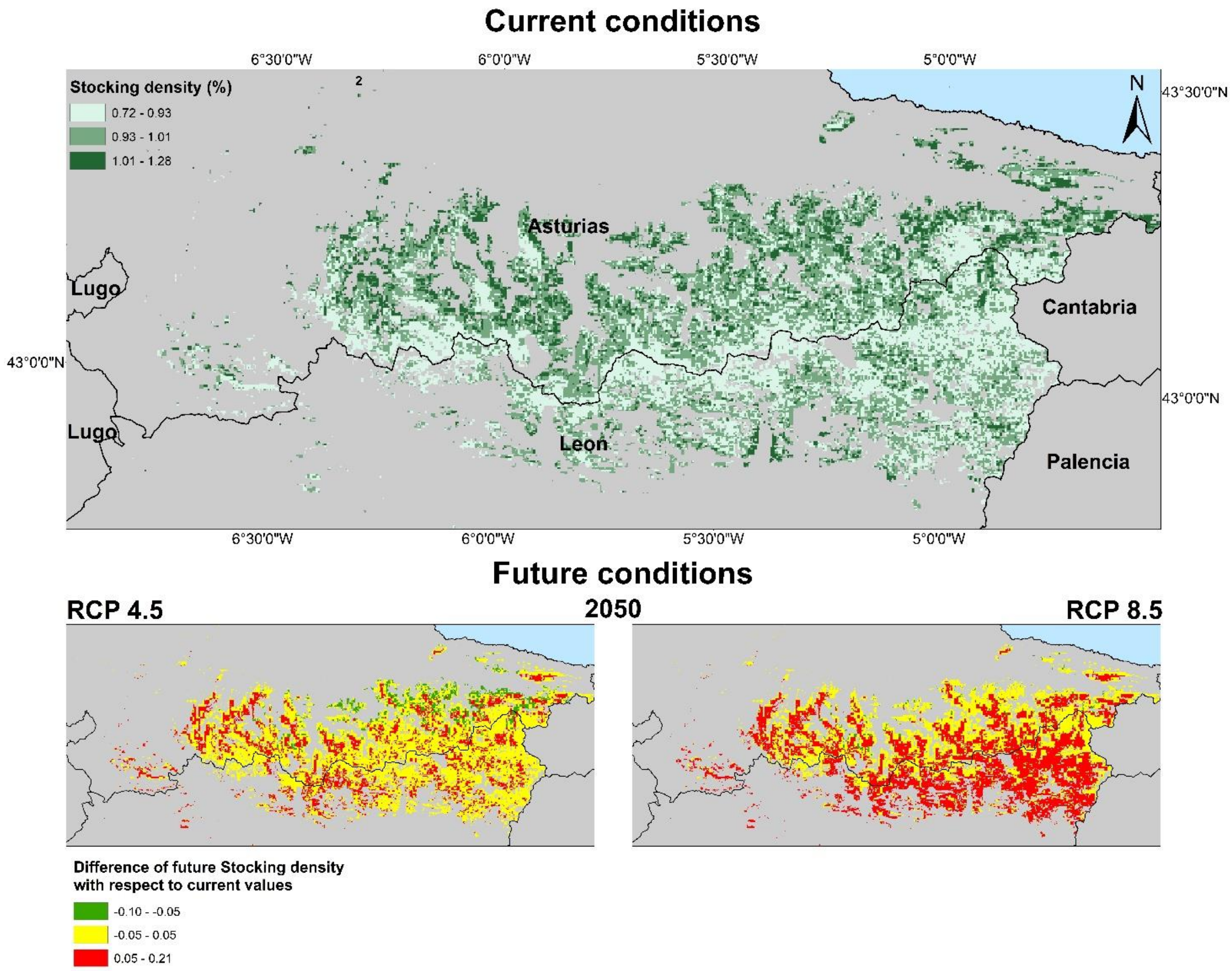

Diversity class: Density and average tree size

<u>RF model</u>: Dominant height